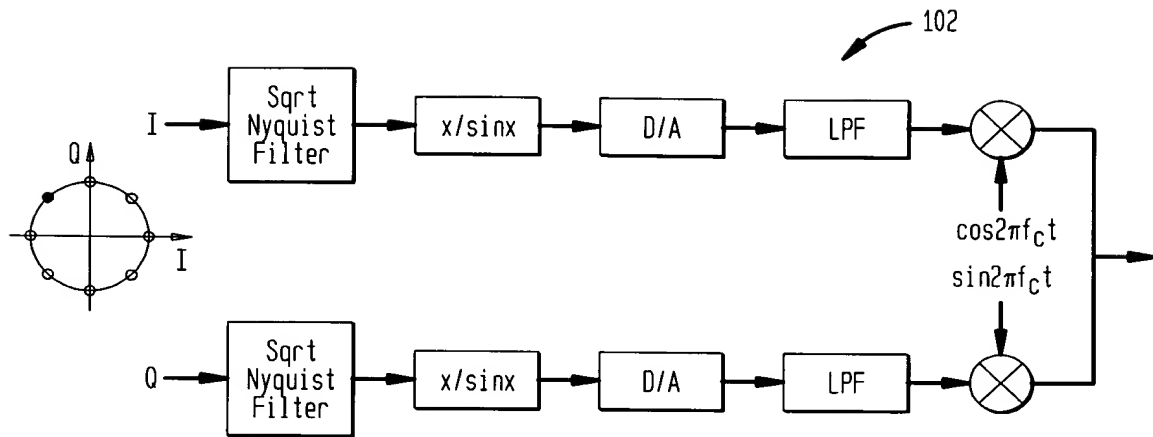


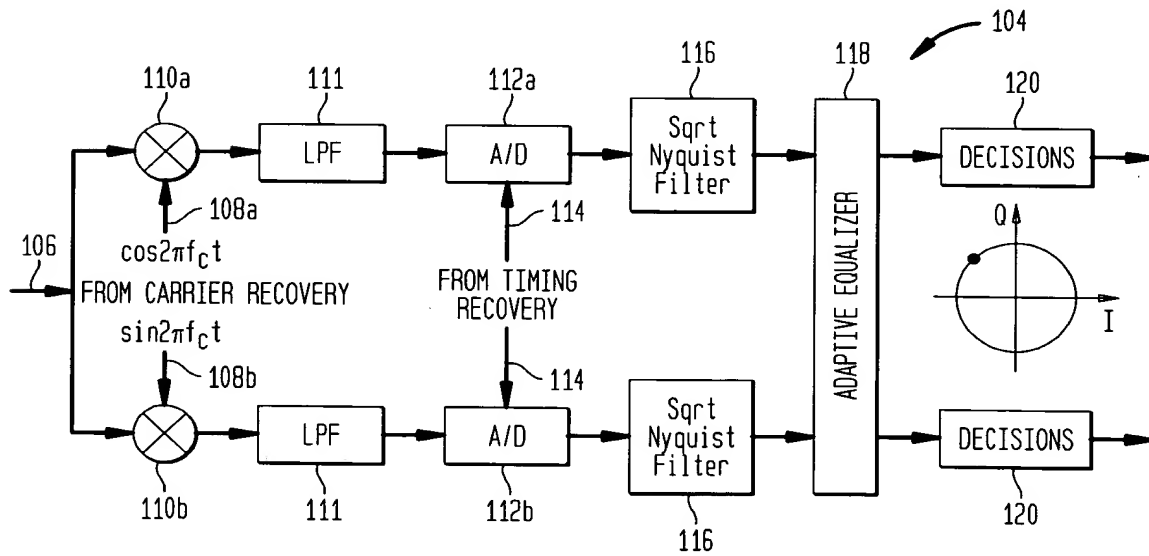


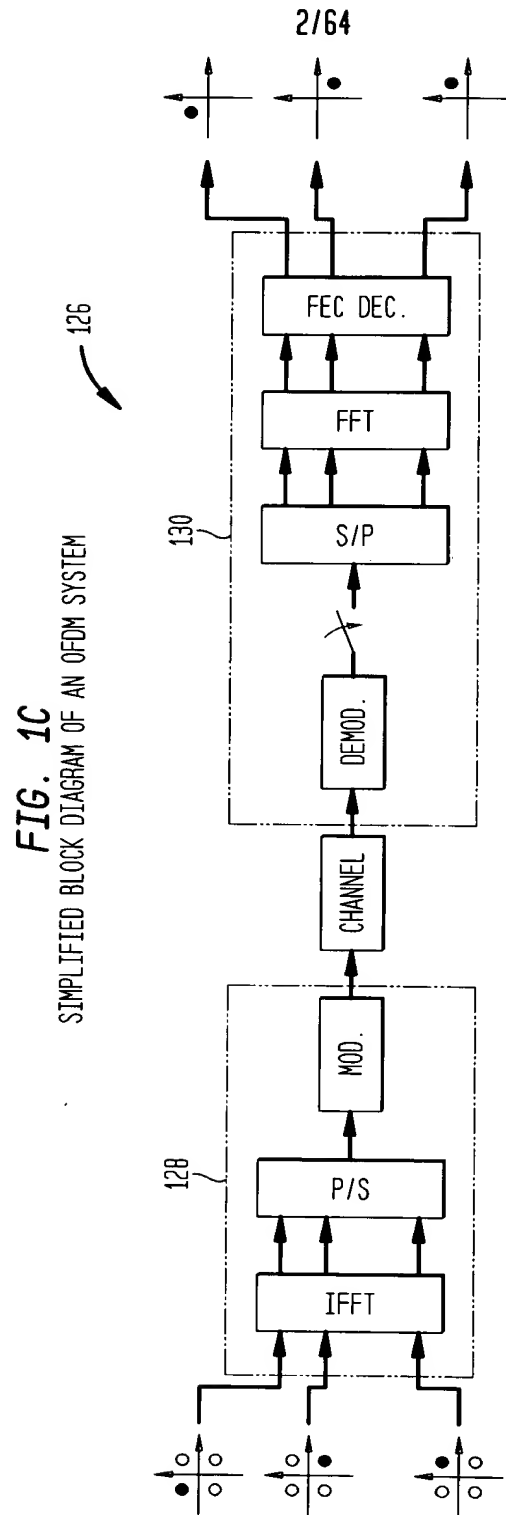
1/64

**FIG. 1A**  
 A SIMPLIFIED PSK TRANSMITTER

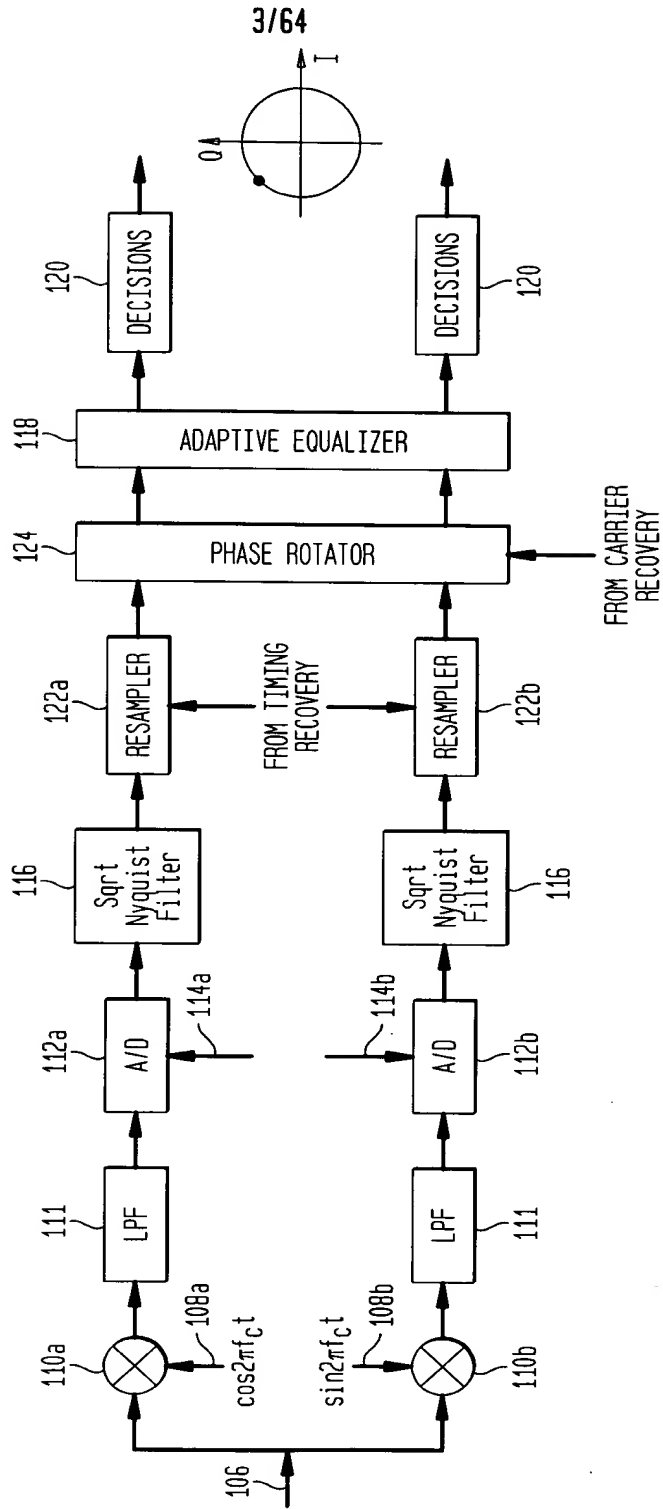


**FIG. 1B**  
 A SIMPLIFIED PSK RECEIVER



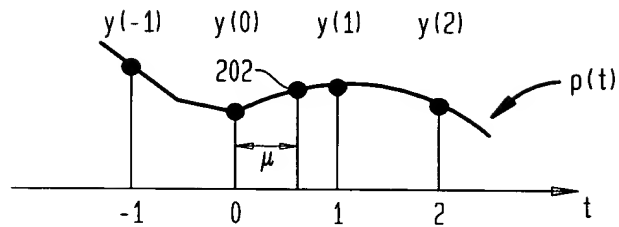


**FIG. 1D**  
 PSK RECEIVER WITH CARRIER AND TIMING RECOVERY

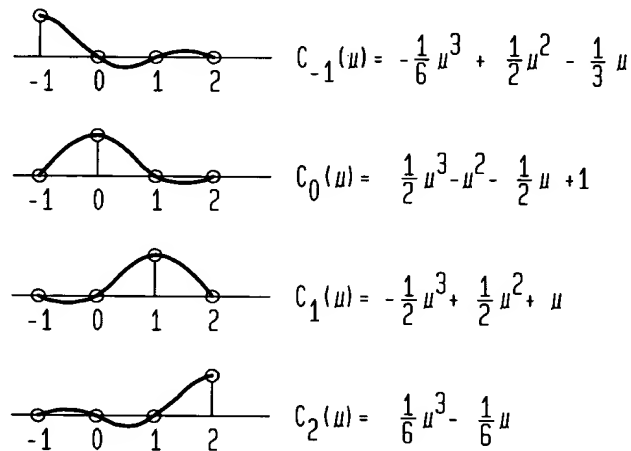


4/64

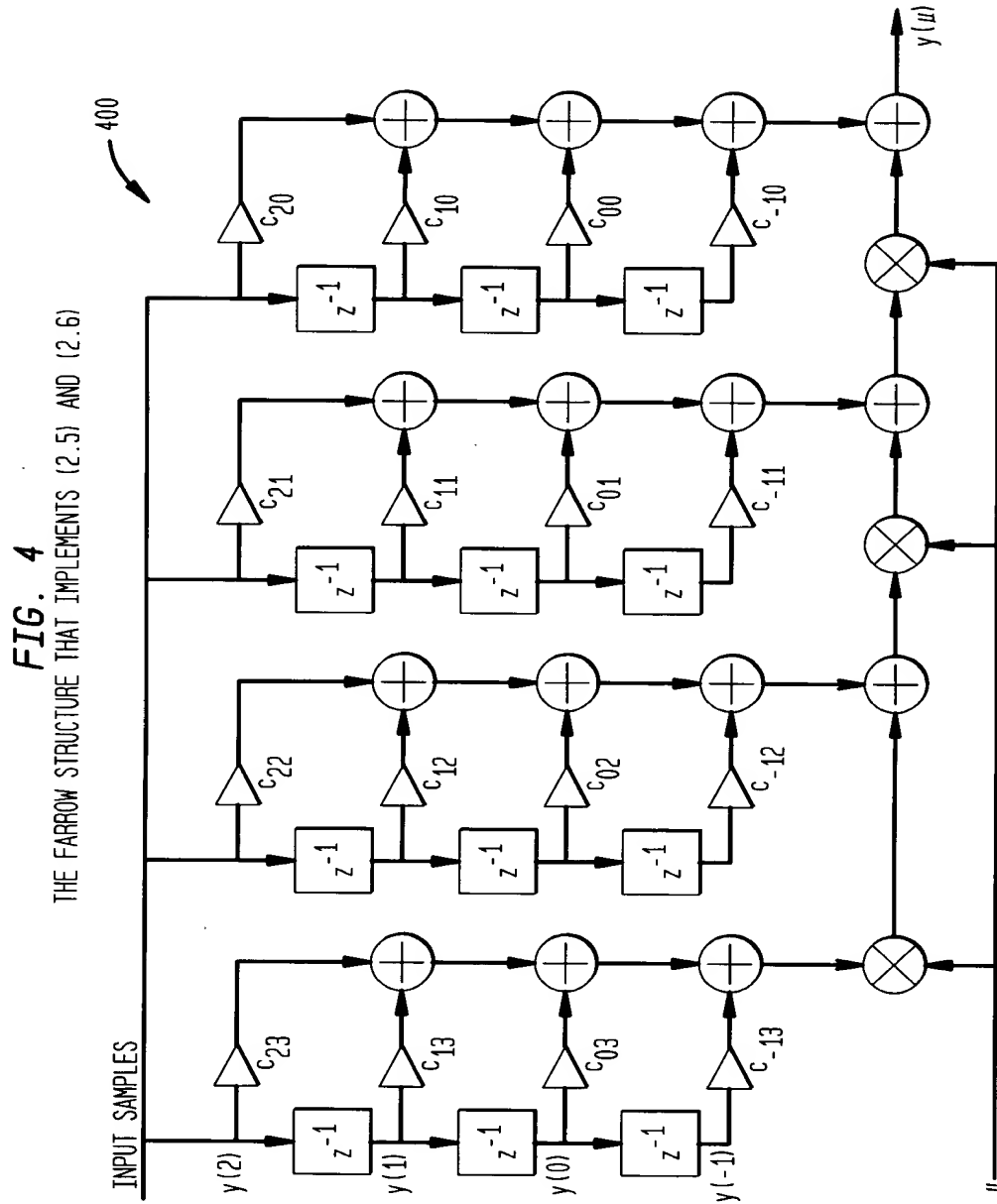
**FIG. 2**  
 INTERPOLATION ENVIRONMENT



**FIG. 3**  
 THE LAGRANGE BASIS POLYNOMIALS

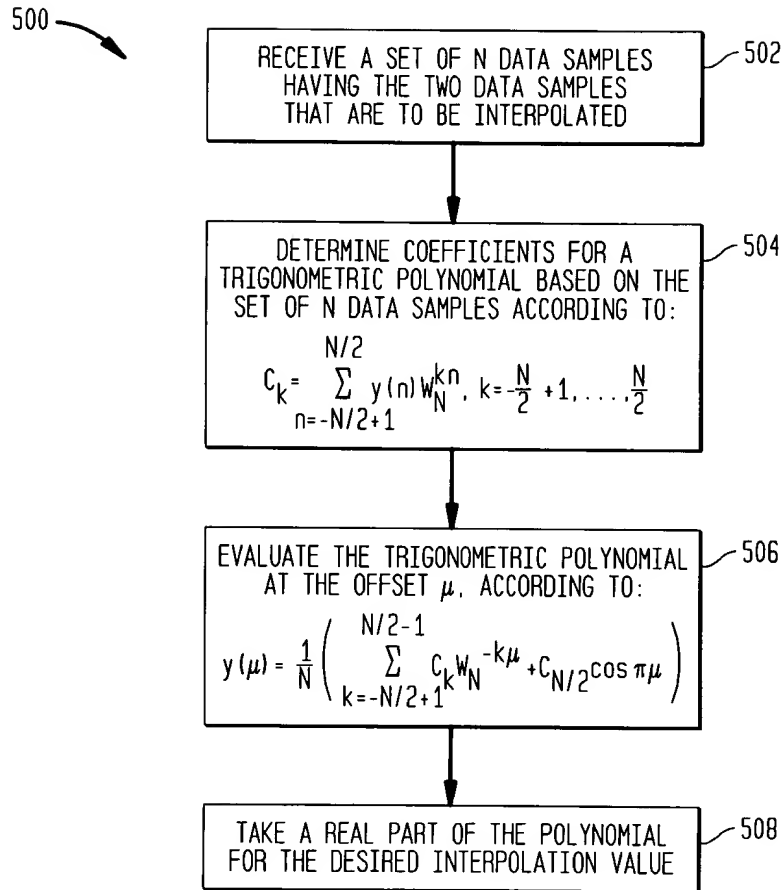


5/64



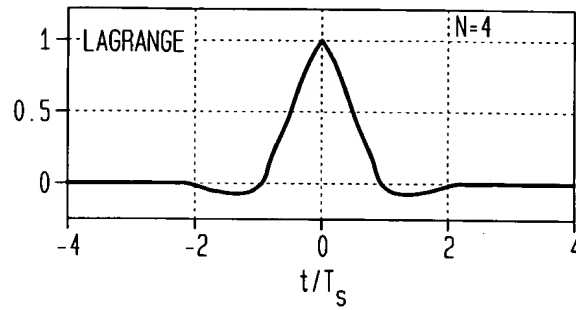
6/64

FIG. 5

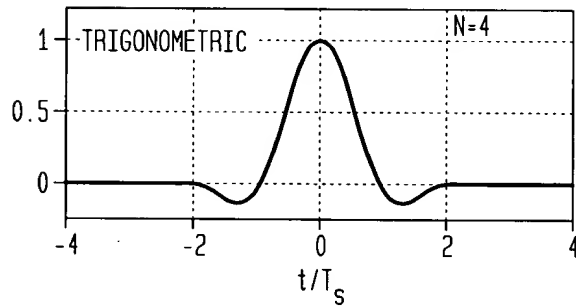


7/64

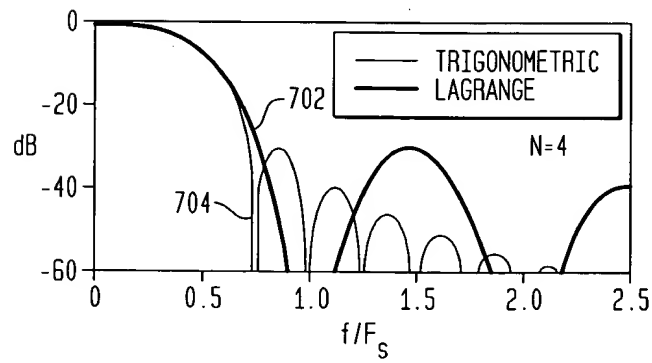
**FIG. 6A**  
IMPULSE RESPONSES OF LAGRANGE INTERPOLATOR



**FIG. 6B**  
IMPULSE RESPONSES OF TRIGONOMETRIC INTERPOLATOR



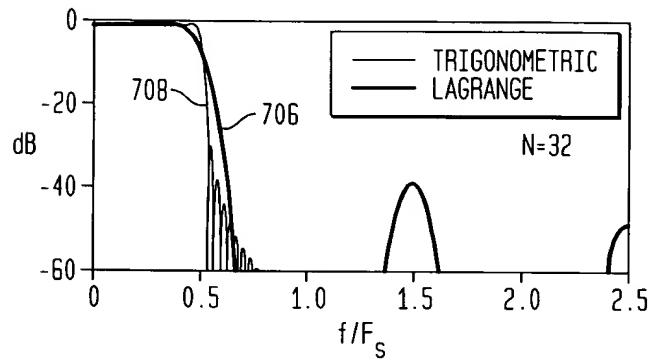
**FIG. 7A**  
FREQUENCY RESPONSES FOR  $N=4$



8/64

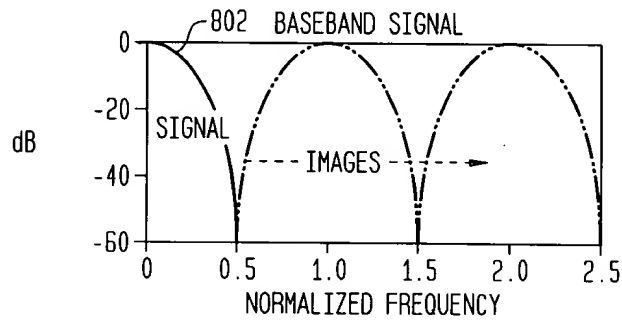
**FIG. 7B**

FREQUENCY RESPONSES FOR N=32



**FIG. 8A**

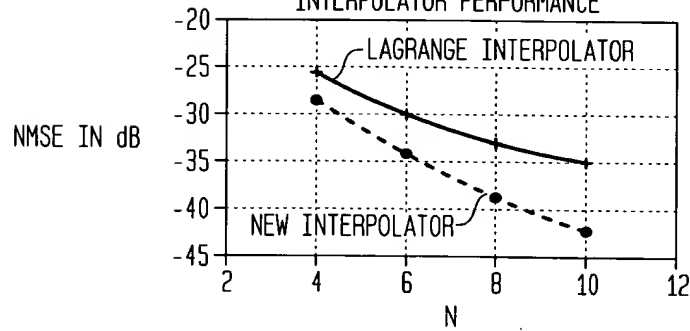
SIGNAL WITH TWO SAMPLES/SYMBOL AND 100% EXCESS BW



**FIG. 8B**

NMSE OF THE INTERPOLATED SIGNAL

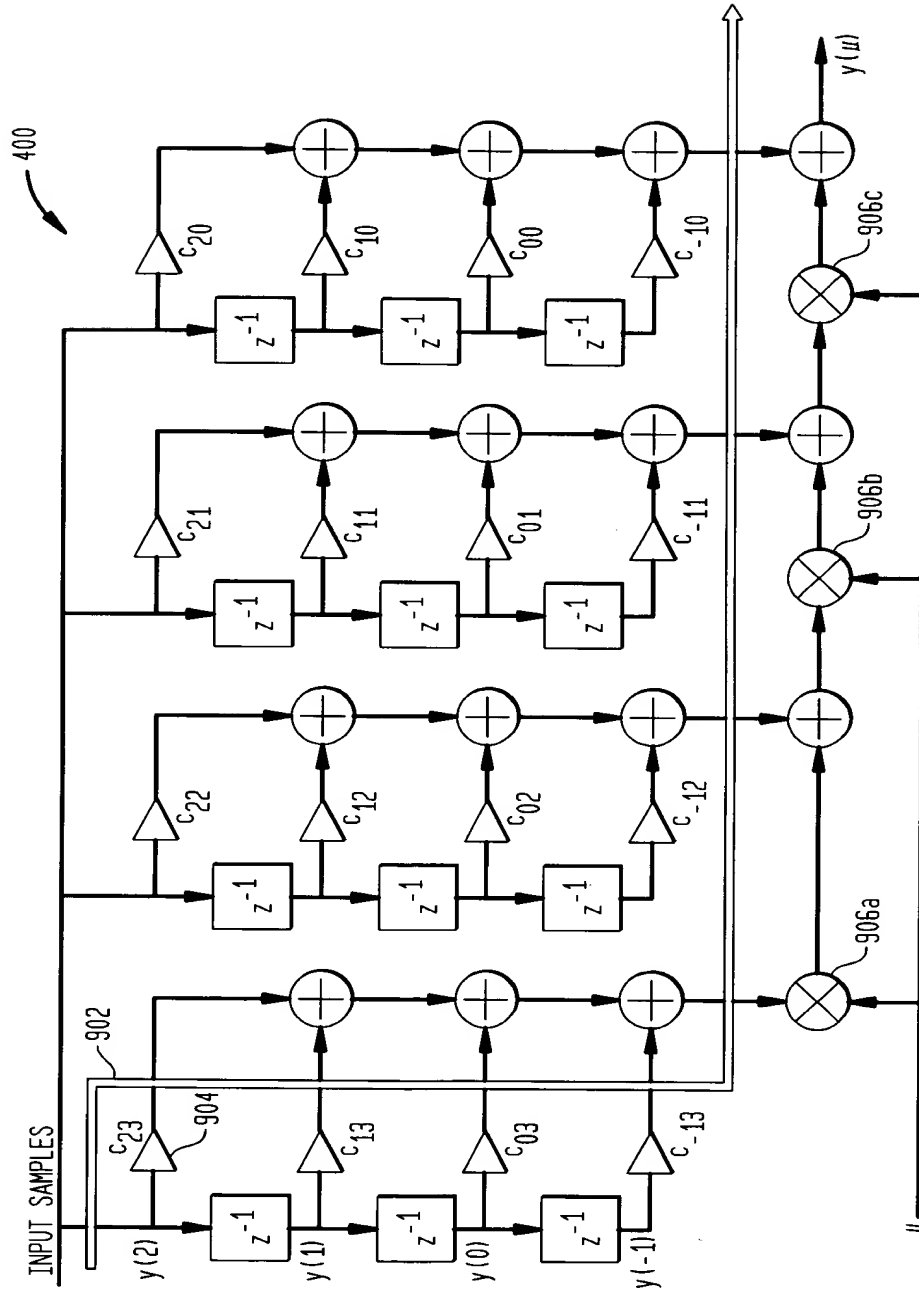
INTERPOLATOR PERFORMANCE





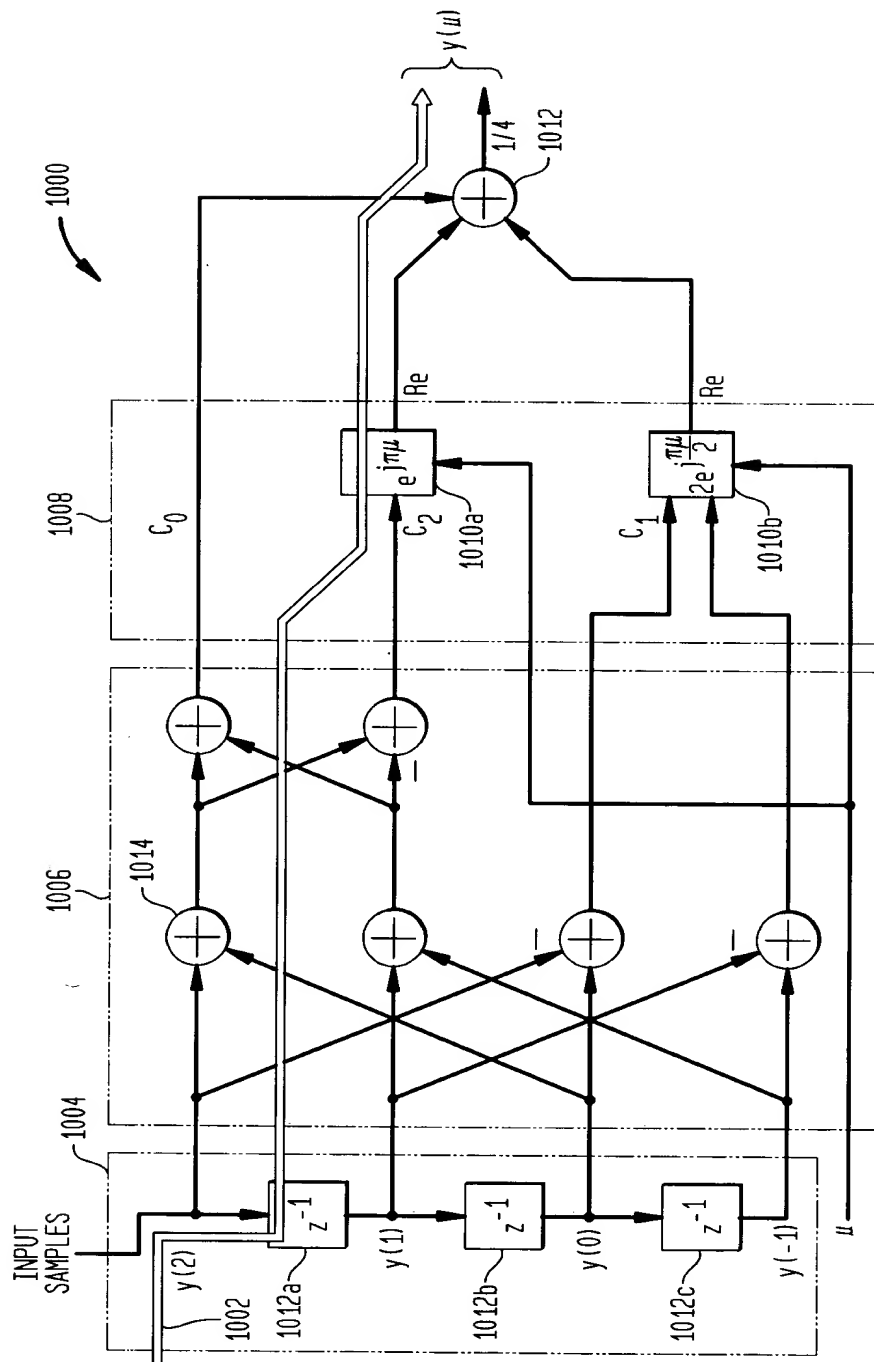
9/64

**FIG. 9**  
 THE CRITICAL PATH OF THE LAGRANGE CUBIC INTERPOLATOR

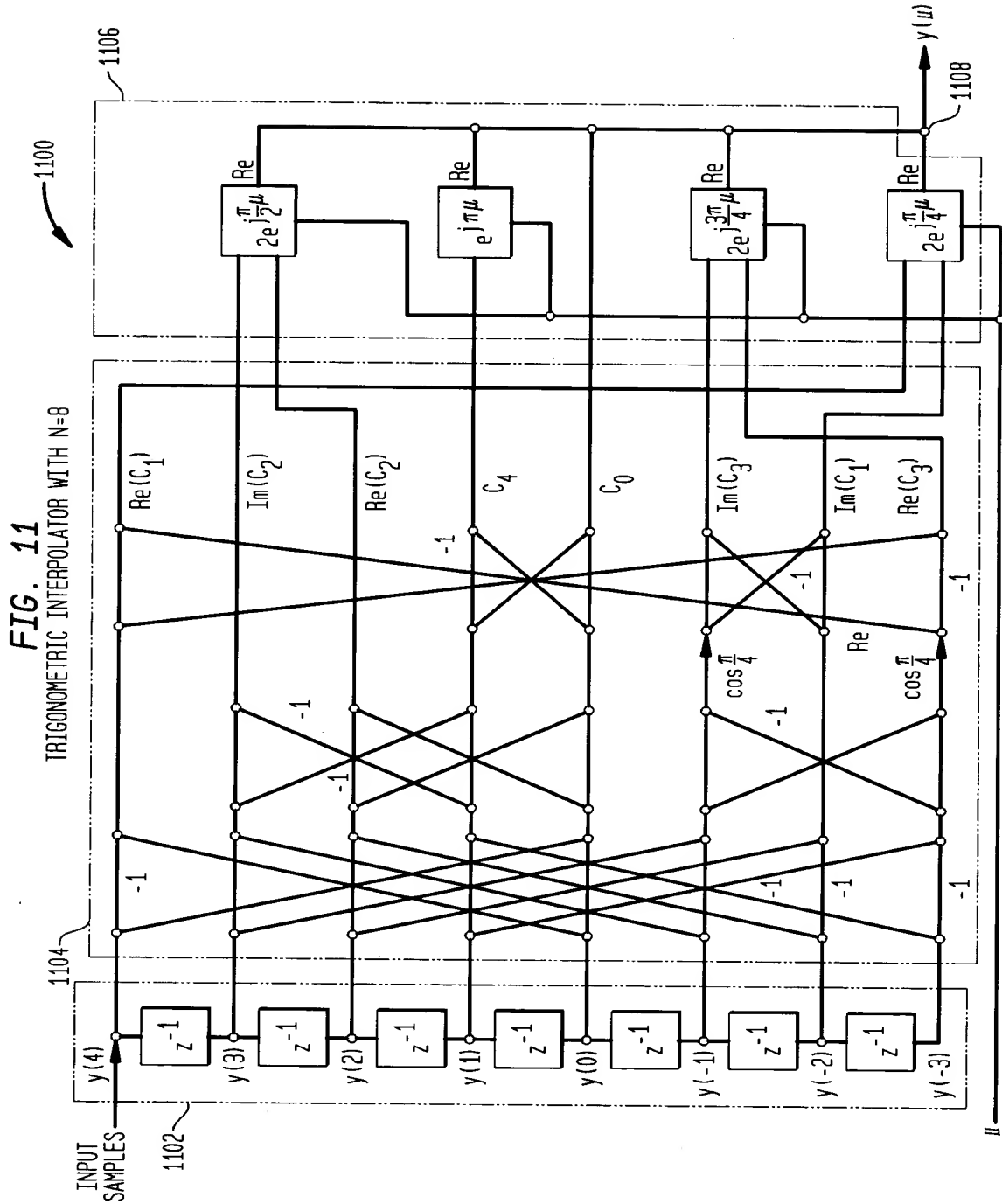


10/64

FIG. 10  
 TRIGONOMETRIC INTERPOLATOR (N=4)

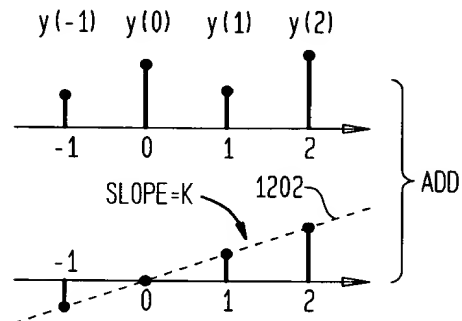


11/64

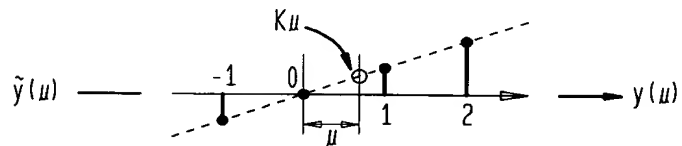


12/64

**FIG. 12**  
 CONCEPTUAL MODIFICATION OF INPUT SAMPLES

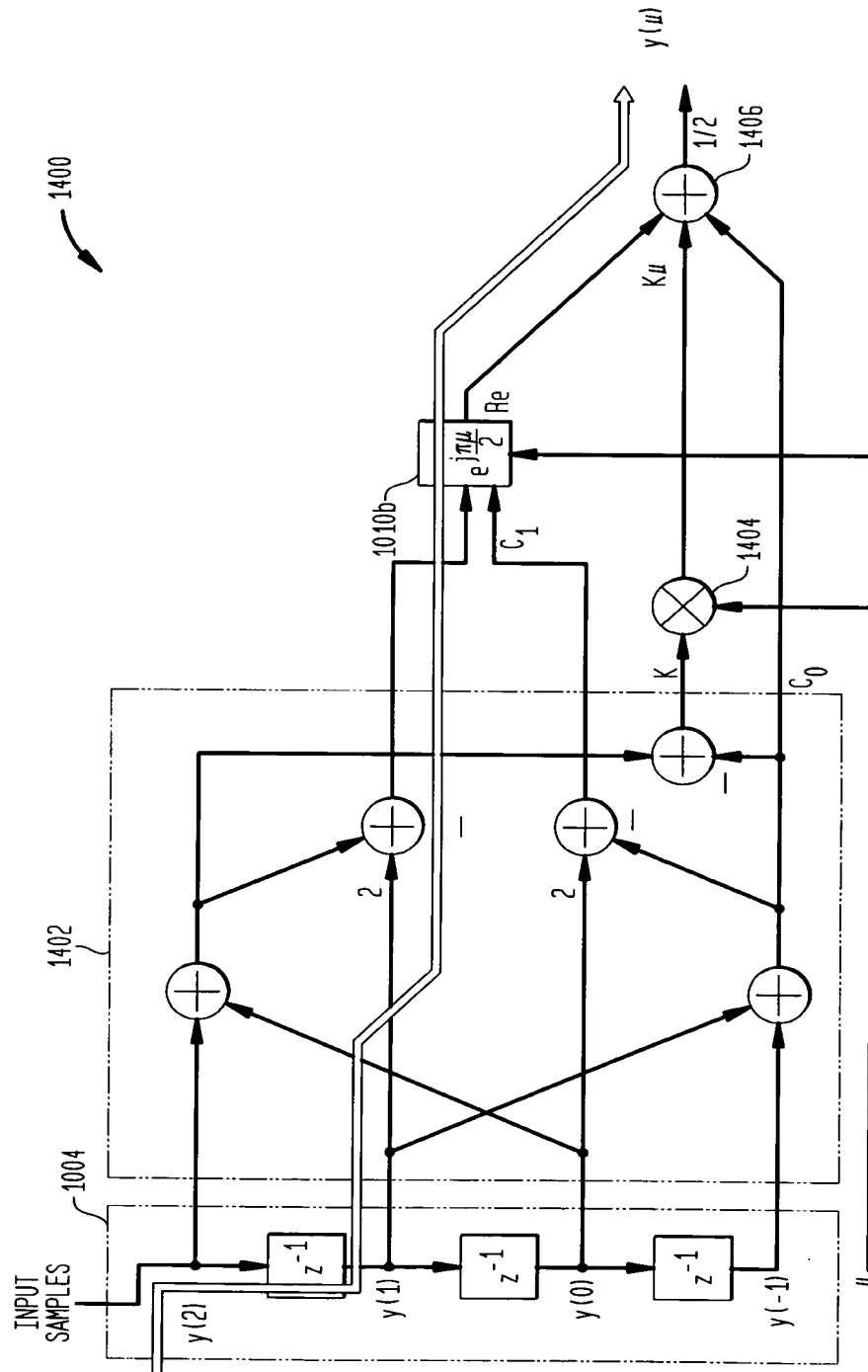


**FIG. 13**  
 CORRECTING THE OFFSET DUE TO MODIFICATION OF ORIGINAL SAMPLES



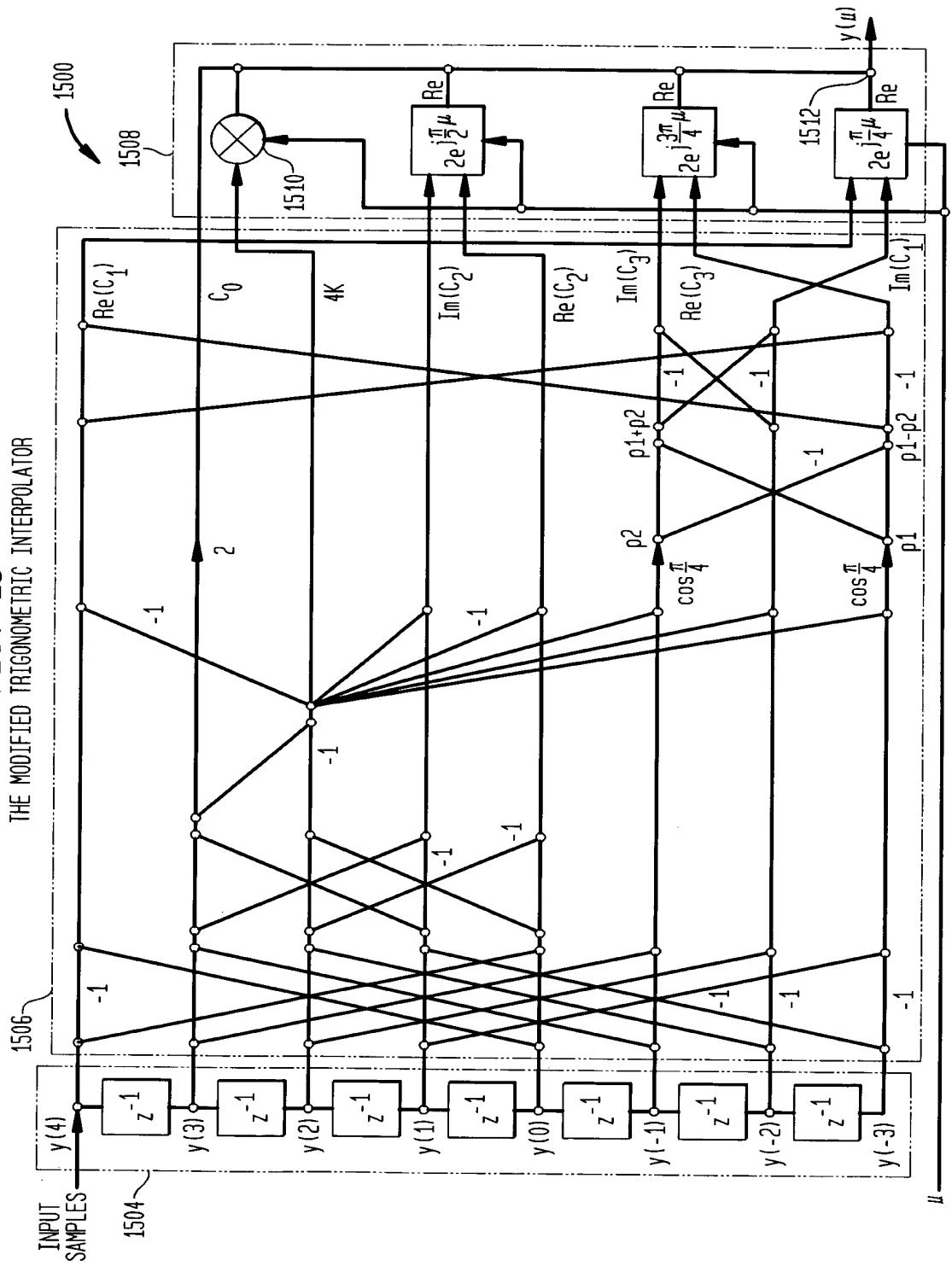
13/64

FIG. 14  
 TRIGONOMETRIC INTERPOLATOR N=4



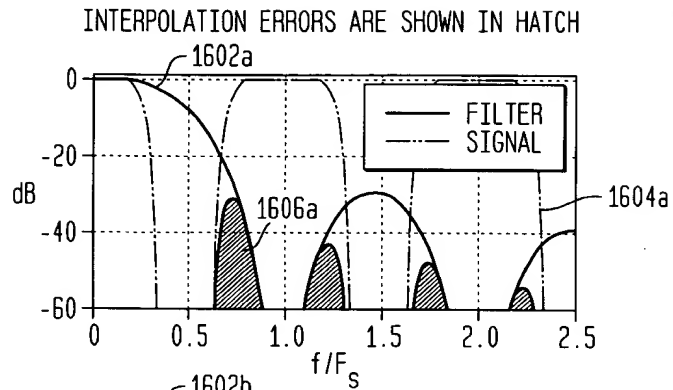
14/64

FIG. 15  
 THE MODIFIED TRIGONOMETRIC INTERPOLATOR

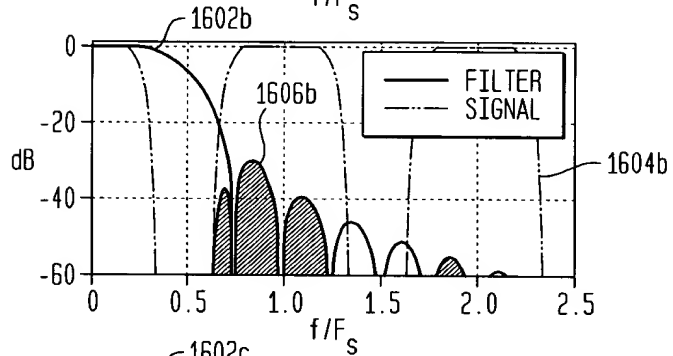


15/64

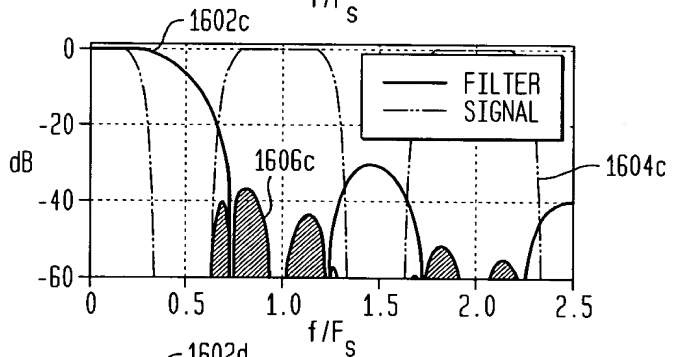
**FIG. 16A**  
 LAGRANGE CUBIC



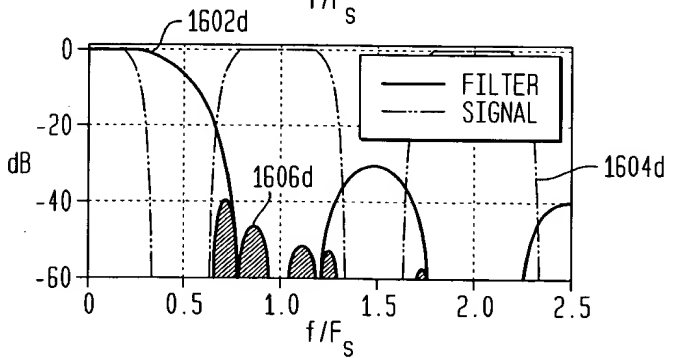
**FIG. 16B**  
 TRIGONOMETRIC INTERPOLATOR 1000  
 (FIG. 10)



**FIG. 16C**  
 TRIGONOMETRIC INTERPOLATOR 1400  
 (FIG. 14)




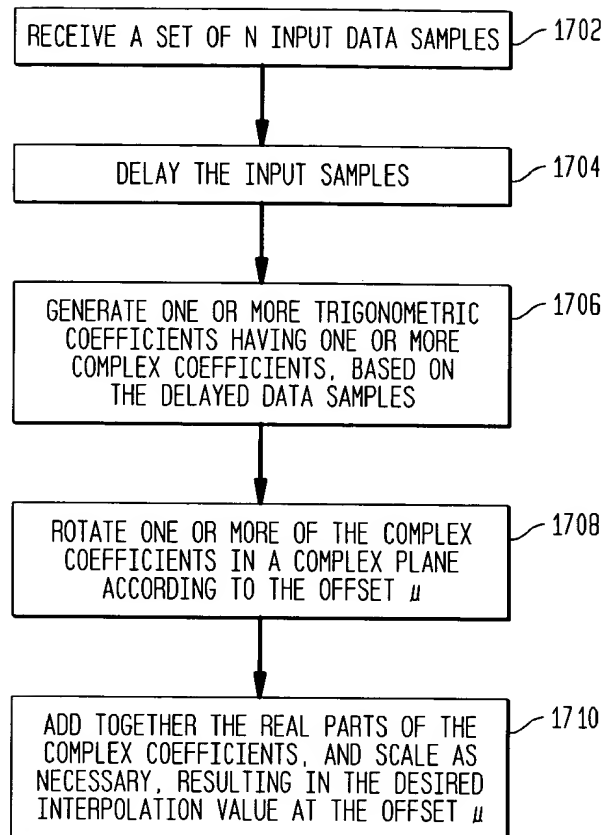
**FIG. 16D**  
 OPTIMAL STRUCTURE



16/64

**FIG. 17**

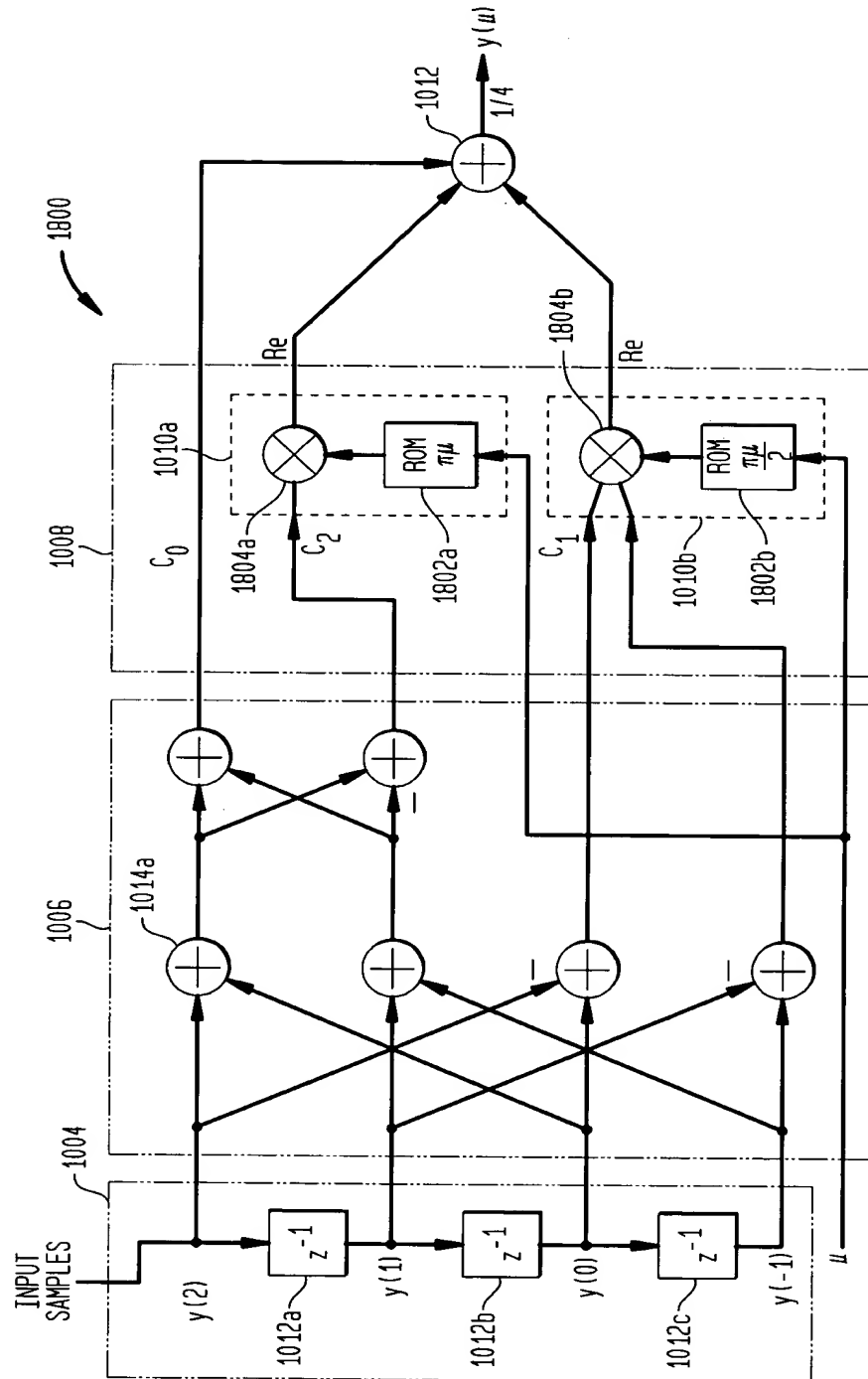
1700 





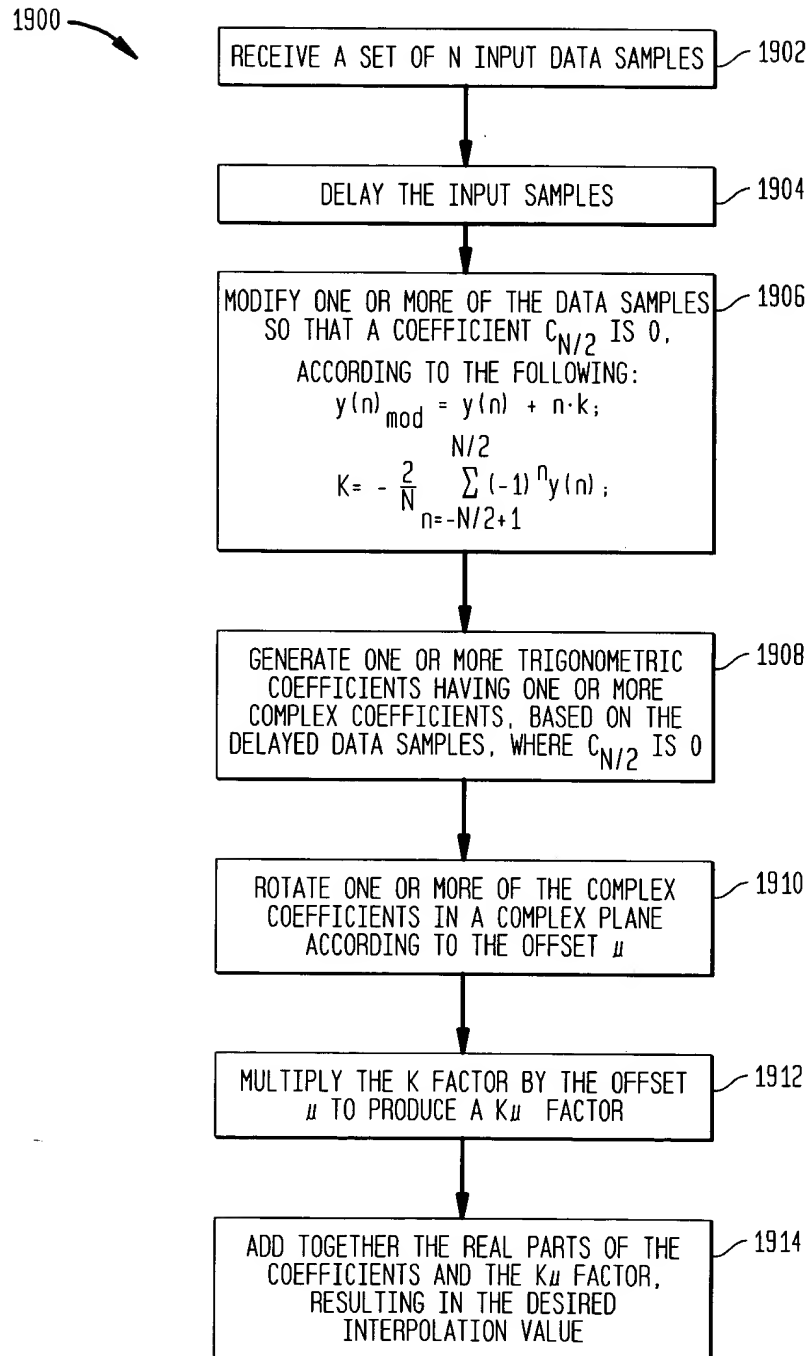
17/64

FIG. 18



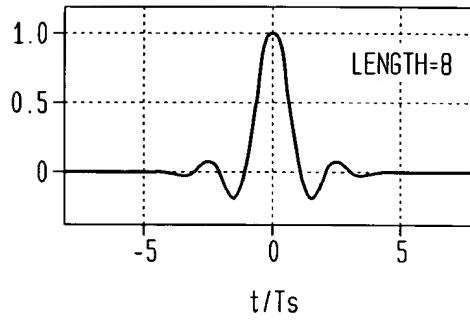
18/64

FIG. 19

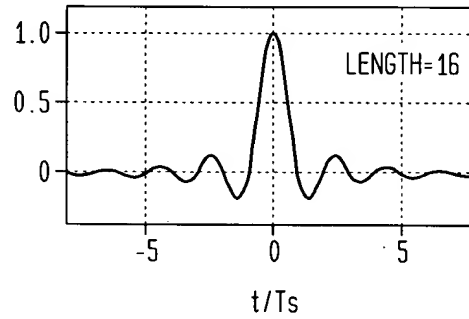


19/64

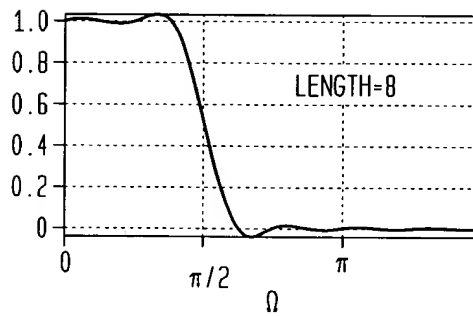
**FIG. 20A**  
NORMALIZED IMPULSE RESPONSES  
f OF THE INTERPOLATION FILTERS



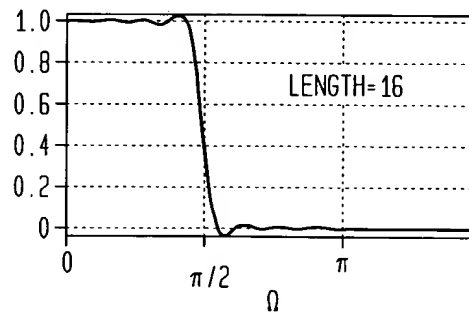
**FIG. 20B**  
NORMALIZED IMPULSE RESPONSES  
f OF THE INTERPOLATION FILTERS



**FIG. 21A**  
NORMALIZED FREQUENCY RESPONSES  
F OF THE INTERPOLATION FILTERS

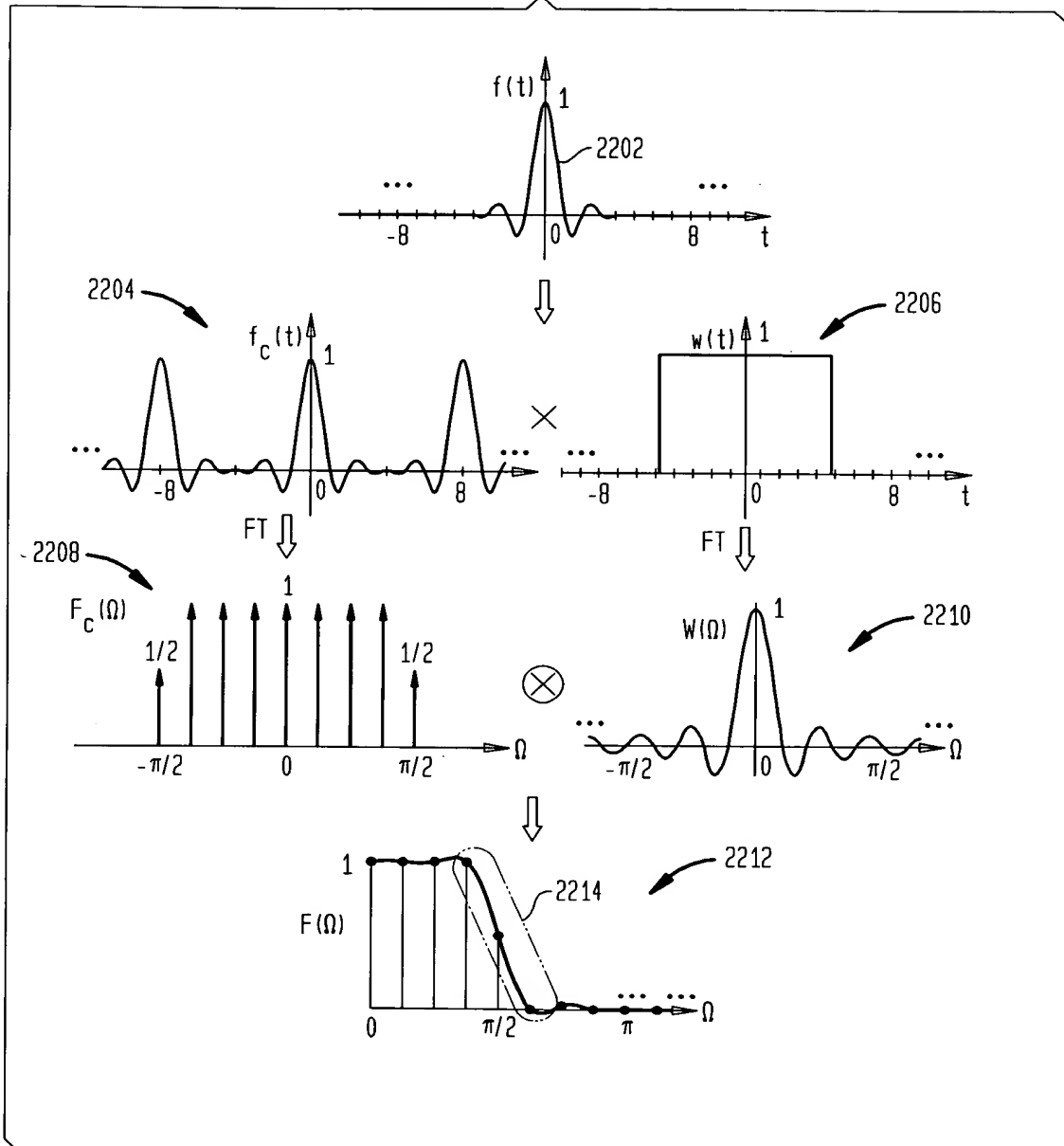


**FIG. 21B**  
NORMALIZED FREQUENCY RESPONSES  
F OF THE INTERPOLATION FILTERS



20/64

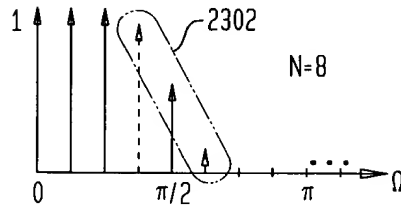
**FIG. 22**  
 ANALYSIS OF THE FREQUENCY RESPONSES



21/64

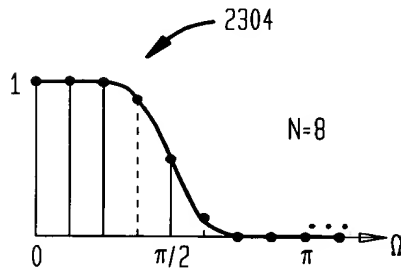
**FIG. 23A**

EFFECT OF A MORE GRADUAL TRANSITION AT THE BAND EDGE



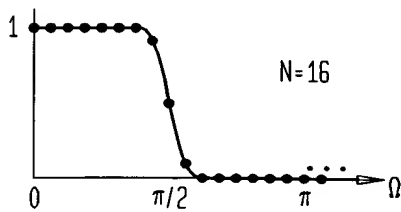
**FIG. 23B**

EFFECT OF A MORE GRADUAL TRANSITION AT THE BAND EDGE



**FIG. 24**

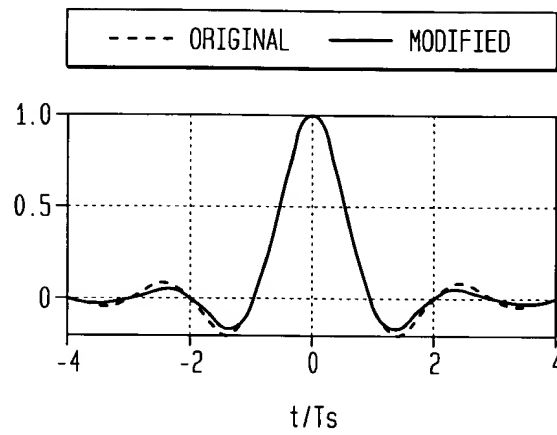
REDUCING THE TRANSITION BANDWIDTH BY INCREASING N



22/64

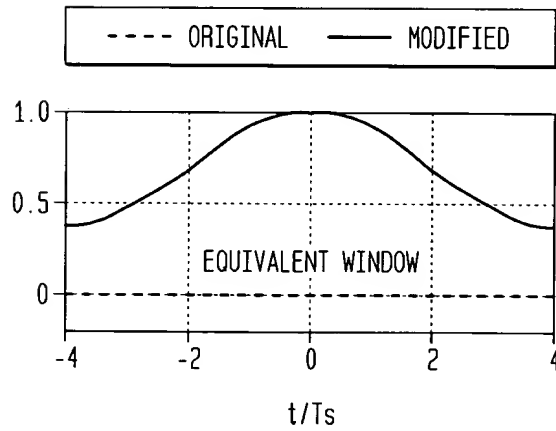
**FIG. 25A**

IMPULSE RESPONSE OF THE ORIGINAL FILTER AND THE MODIFIED FILTER



**FIG. 25B**

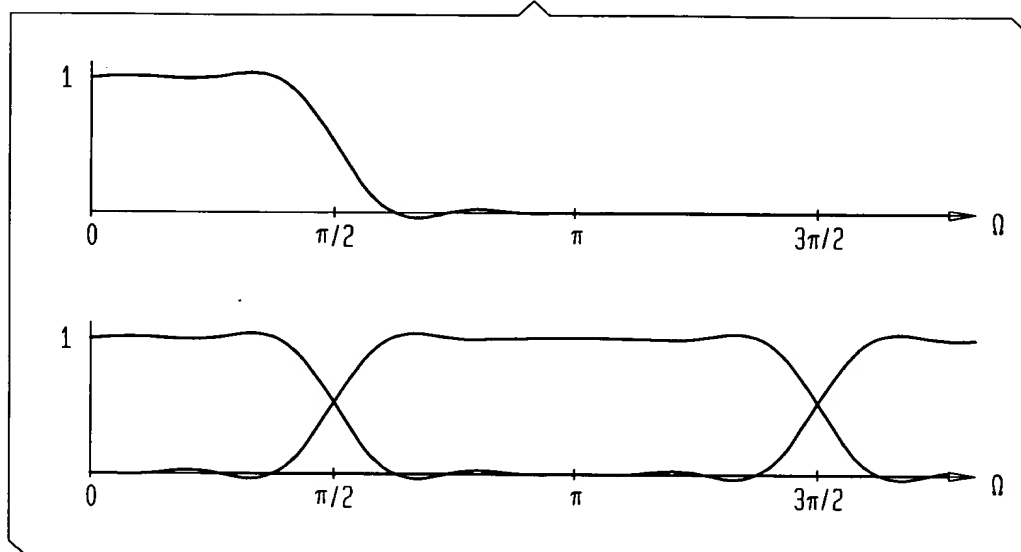
THE EQUIVALENT WINDOW



23/64

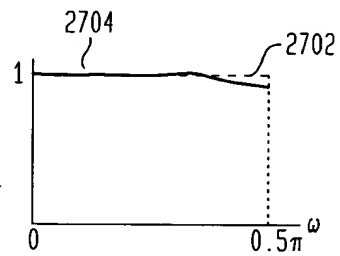
**FIG. 26**

FORMING THE FREQUENCY RESPONSE OF THE  
 DISCRETE-TIME FRACTIONAL-DELAY FILTER



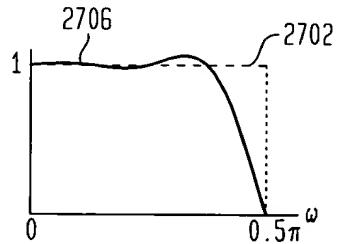
**FIG. 27A**

FRACTIONAL-DELAY FILTER WITH  $\mu=0.12$ ,  
 USING THE PRELIMINARY N=8 INTERPOLATOR



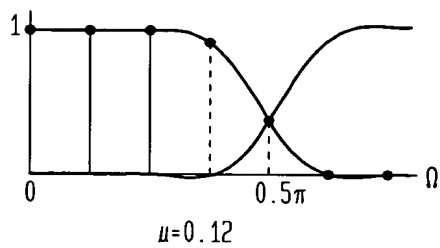
**FIG. 27B**

FRACTIONAL-DELAY FILTER WITH  $\mu=0.5$ ,  
 USING THE PRELIMINARY N=8 INTERPOLATOR

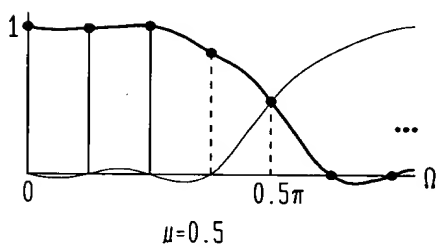


24/64

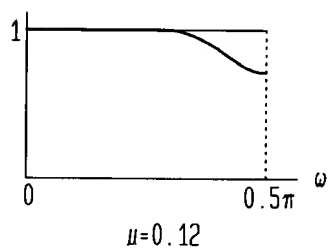
**FIG. 28A**



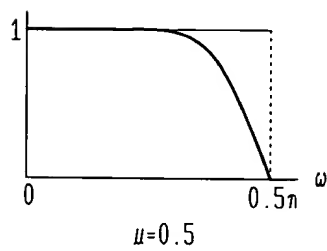
**FIG. 28B**



**FIG. 28C**



**FIG. 28D**

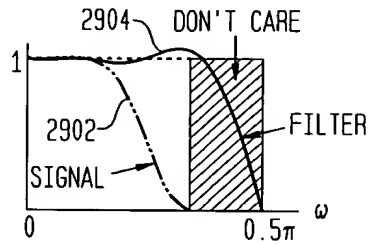




25/64

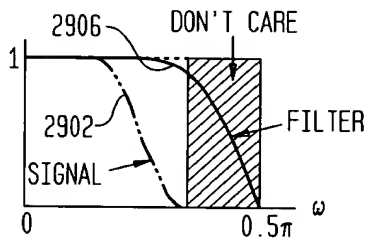
**FIG. 29A**

$F_{\mu}(\omega)$ , WITH  $\mu=0.5$ ,  $N=8$ , BEFORE OPTIMIZATION



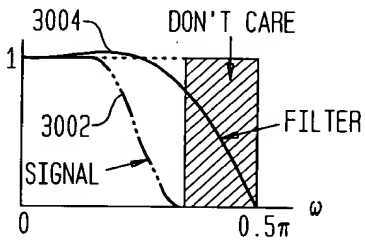
**FIG. 29B**

$F_{\mu}(\omega)$ , WITH  $\mu=0.5$ ,  $N=8$ , AFTER OPTIMIZATION



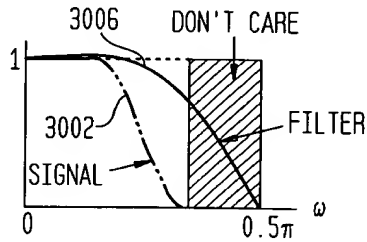
**FIG. 30A**

$F_{\mu}(\omega)$ , WITH  $\mu=0.5$ ,  $N=4$ , BEFORE MODIFICATION



**FIG. 30B**

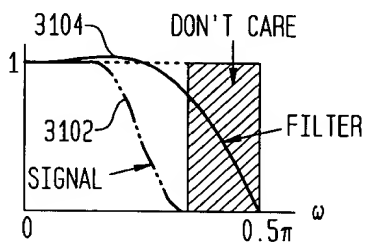
$F_{\mu}(\omega)$ , WITH  $\mu=0.5$ ,  $N=4$ , AFTER MODIFICATION



26/64

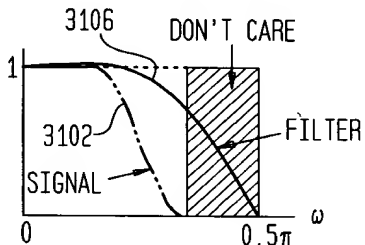
**FIG. 31A**

$F_{\mu}(\omega)$ ,  $\mu=0.5$ , SIMPLIFIED N=4 STRUCTURE BEFORE MODIFICATION



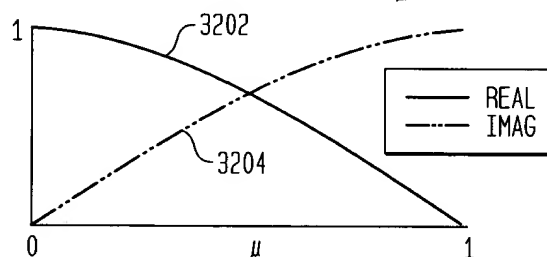
**FIG. 31B**

$F_{\mu}(\omega)$ ,  $\mu=0.5$ , SIMPLIFIED N=4 STRUCTURE AFTER MODIFICATION



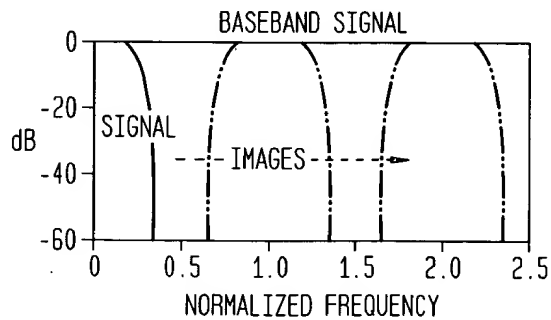
**FIG. 32**

REAL AND IMAGINARY COMPONENTS OF THE  $F_{\mu}(1)e^{j\frac{\pi}{2}\mu}$  VALUE



**FIG. 33**

SIGNAL WITH TWO SAMPLES/SYMBOL AND 40% EXCESS BANDWIDTH



27/64

FIG. 34

3400 →

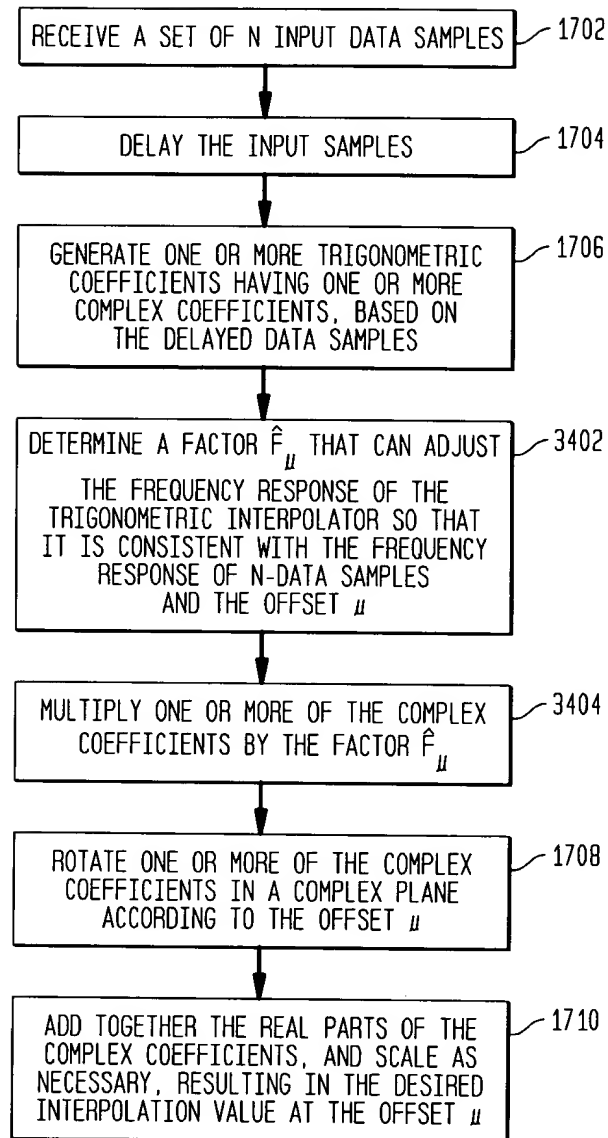
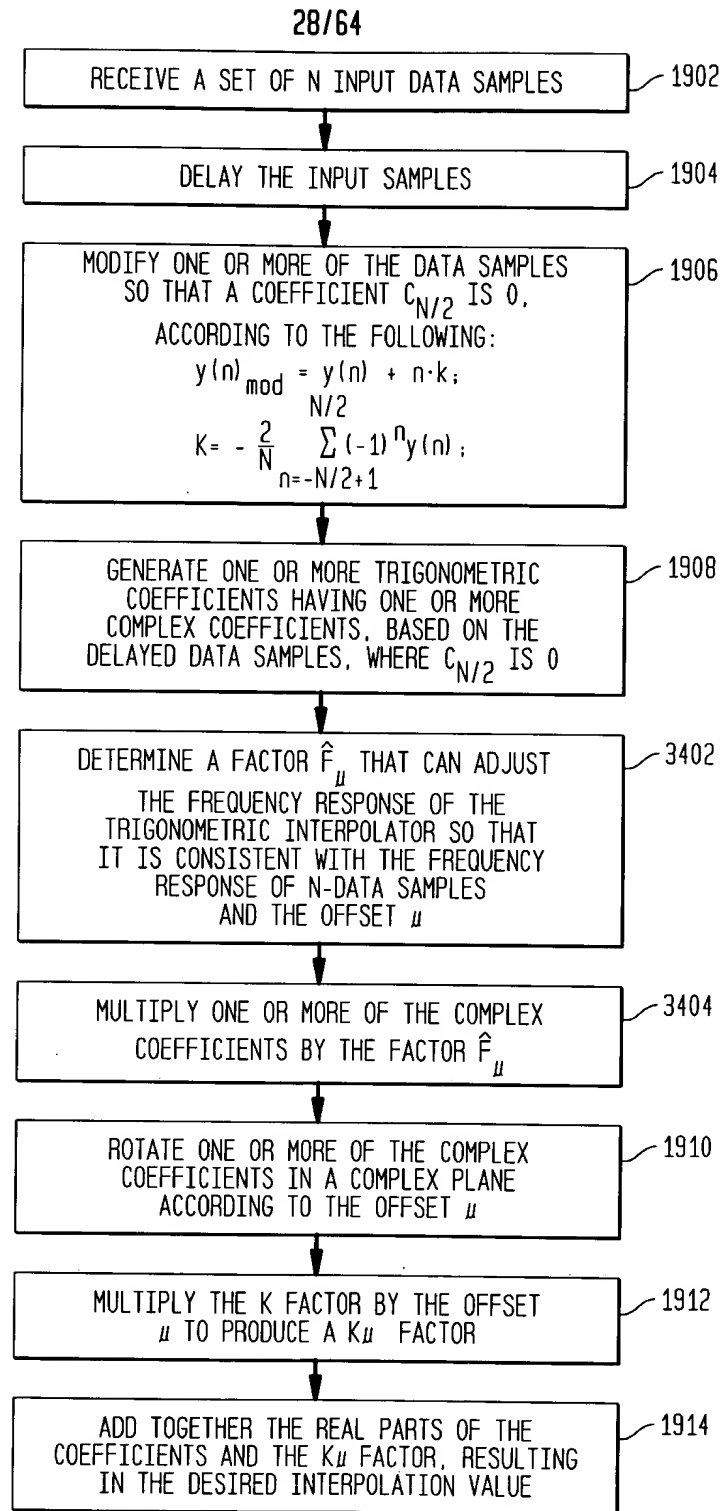


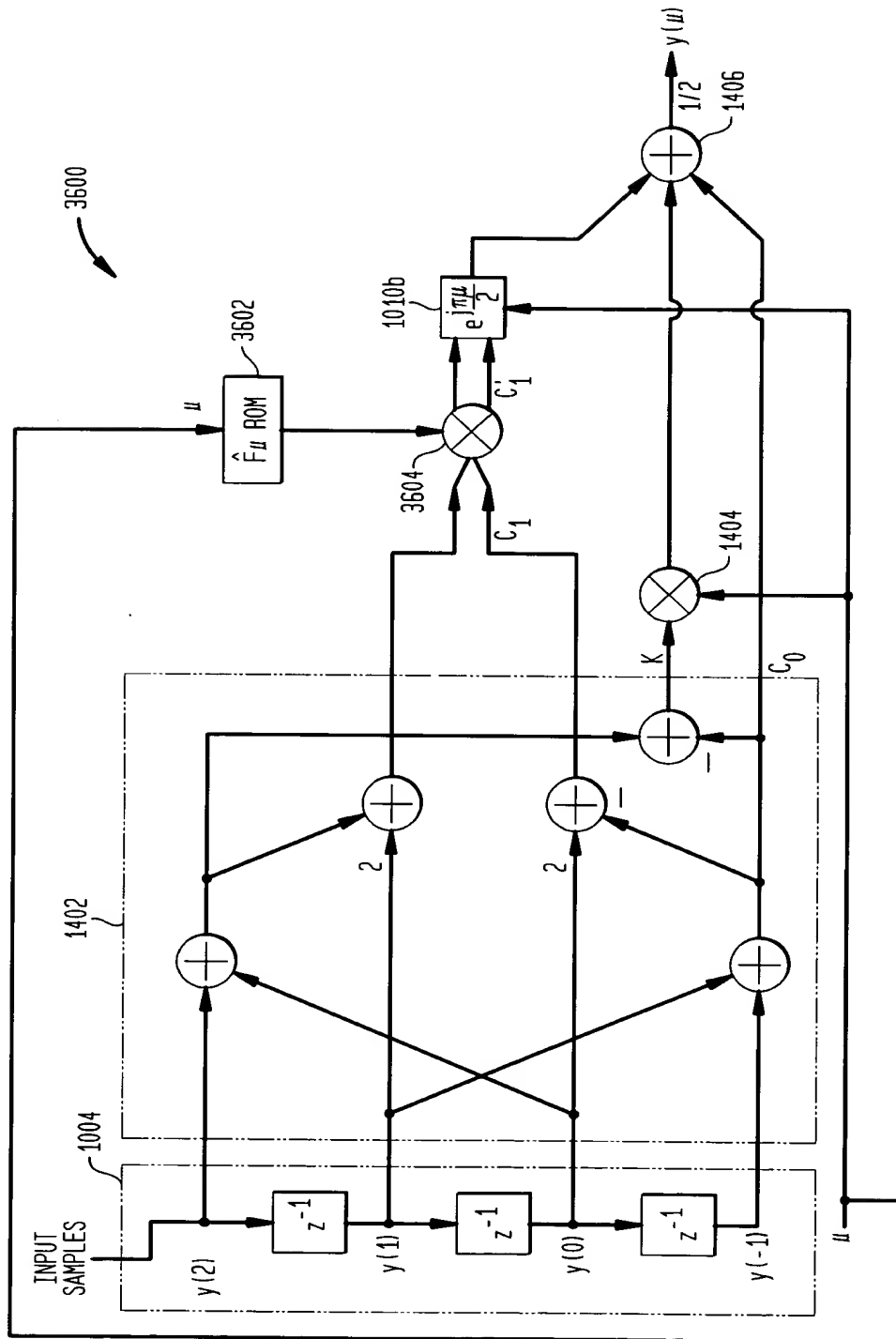
FIG. 35

3500



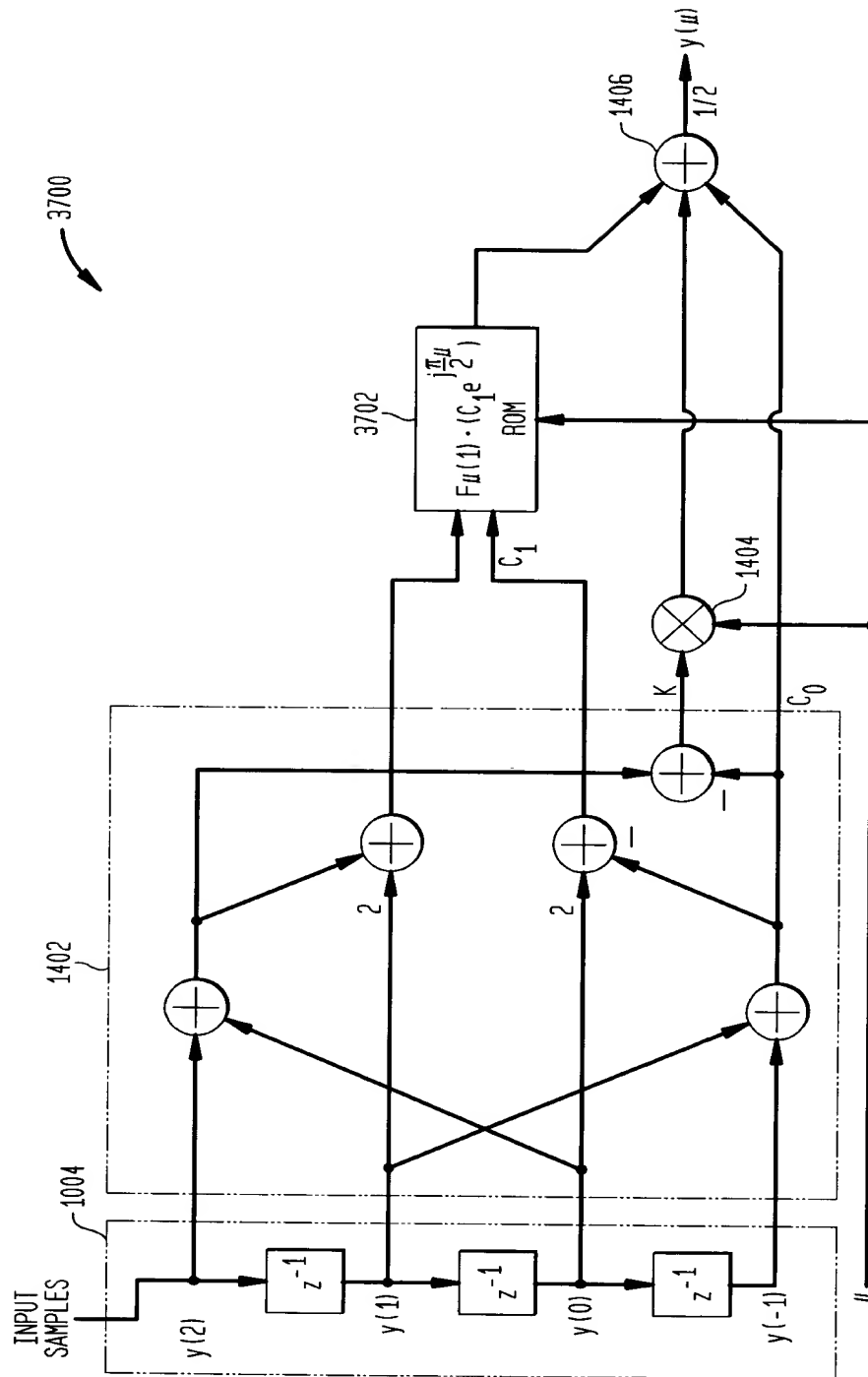
29/64

FIG. 36  
 THE OPTIMIZED STRUCTURE FOR N=4

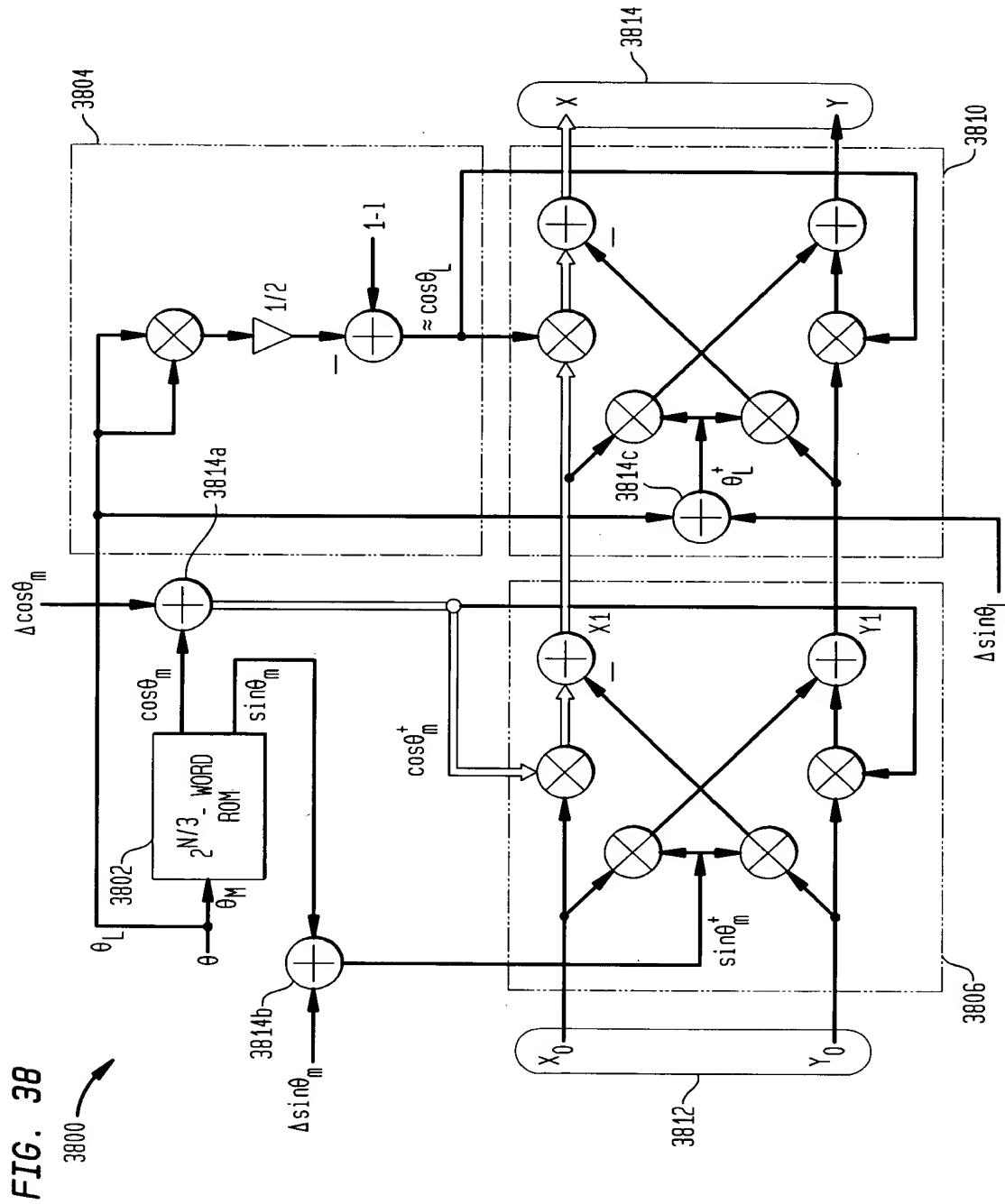


30/64

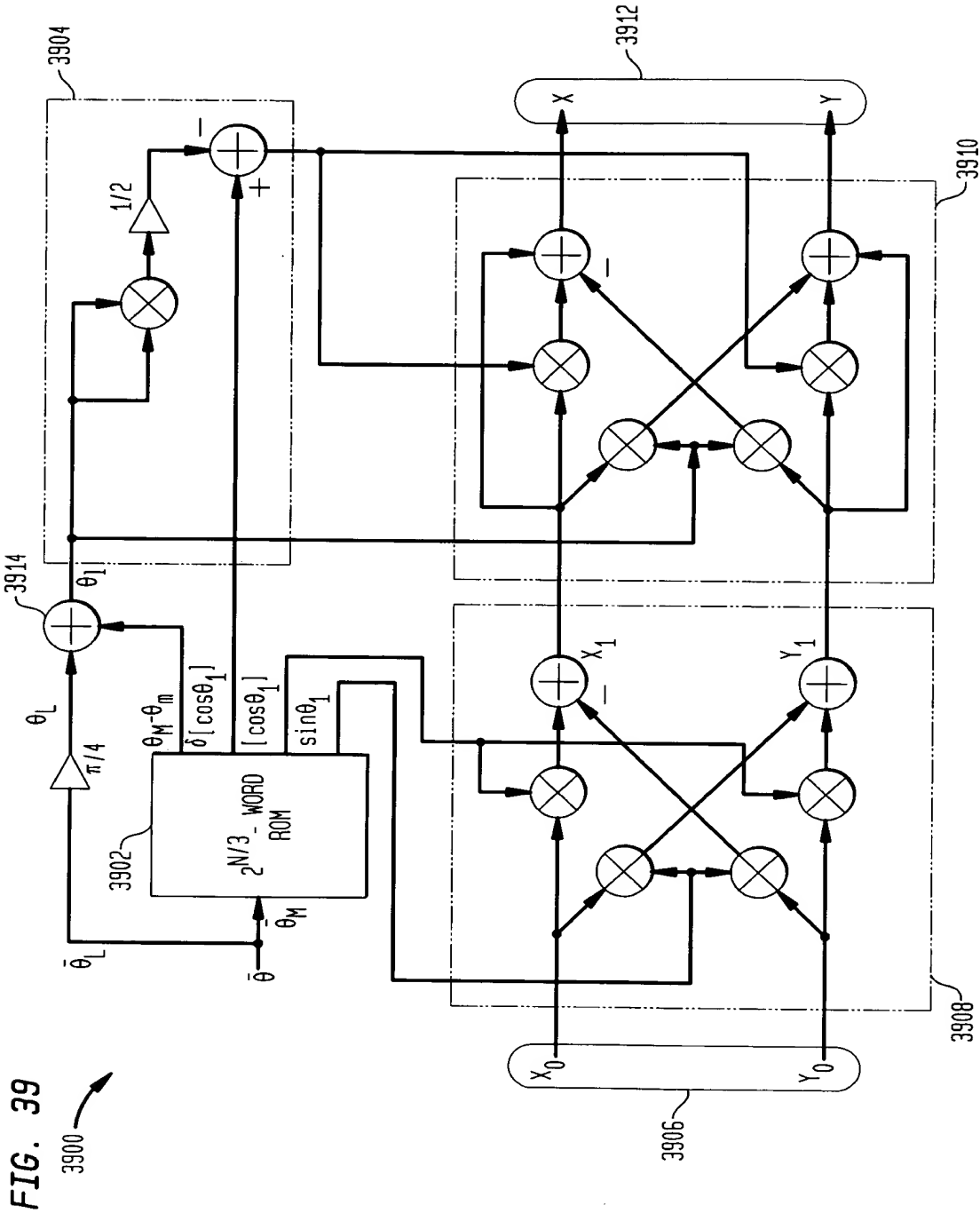
FIG. 37  
 THE OPTIMIZED STRUCTURE FOR N=4



31/64

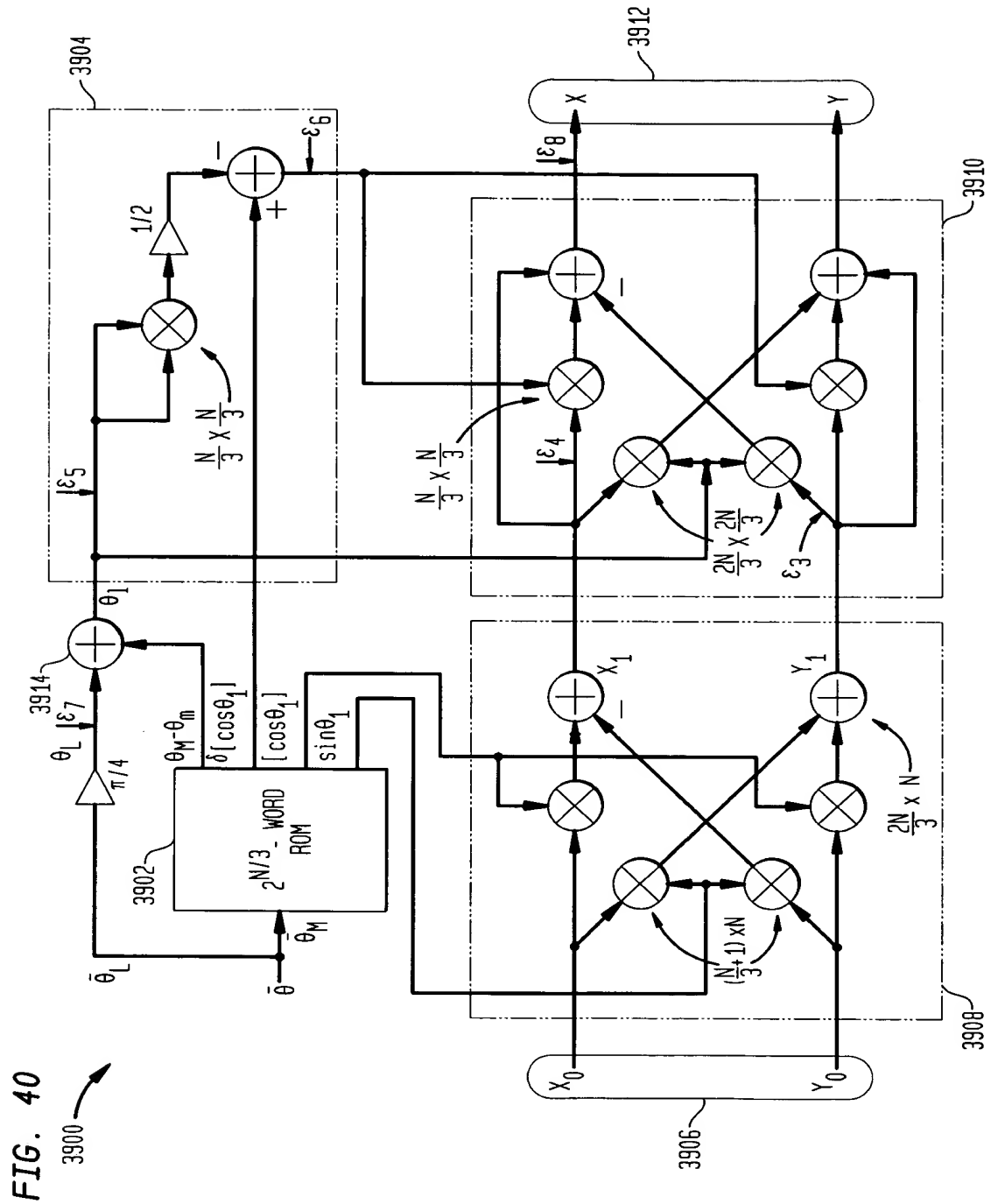


32/64



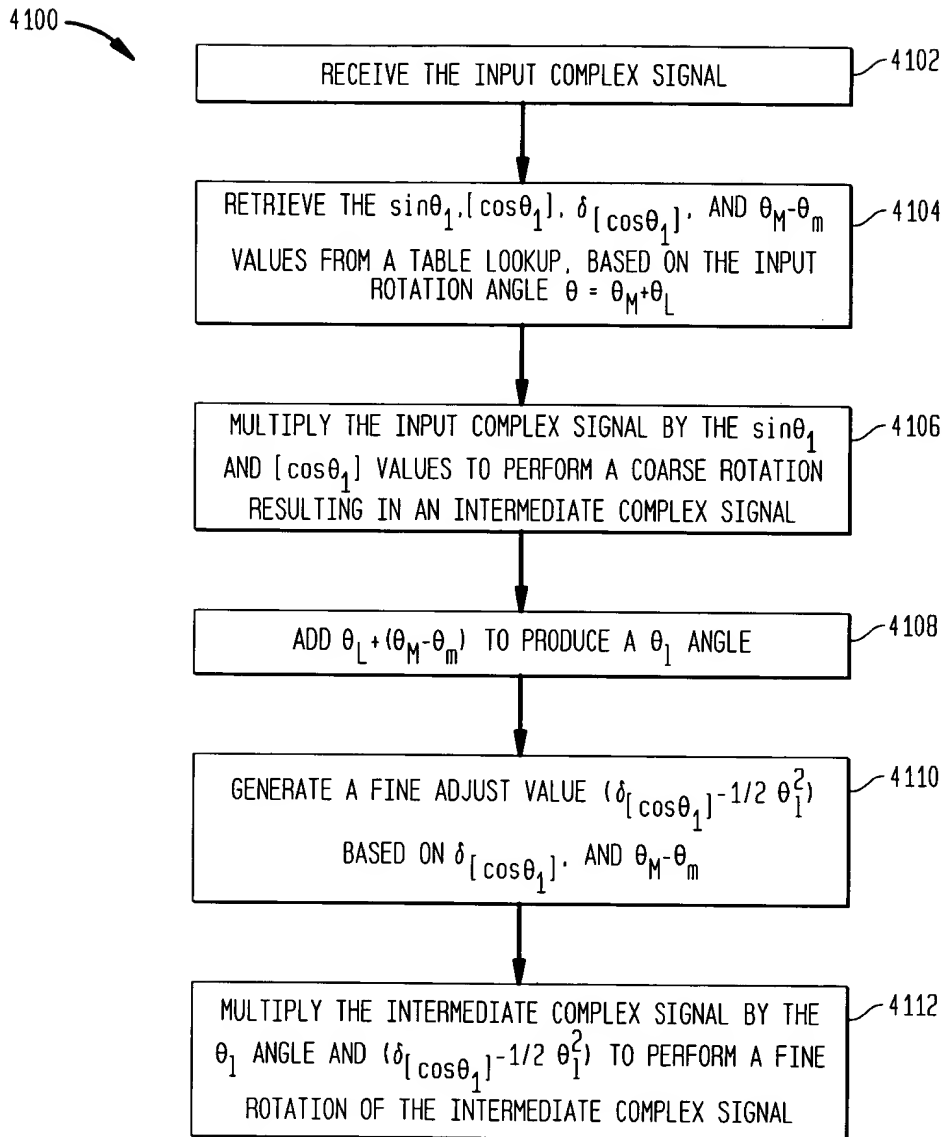


33/64



34/64

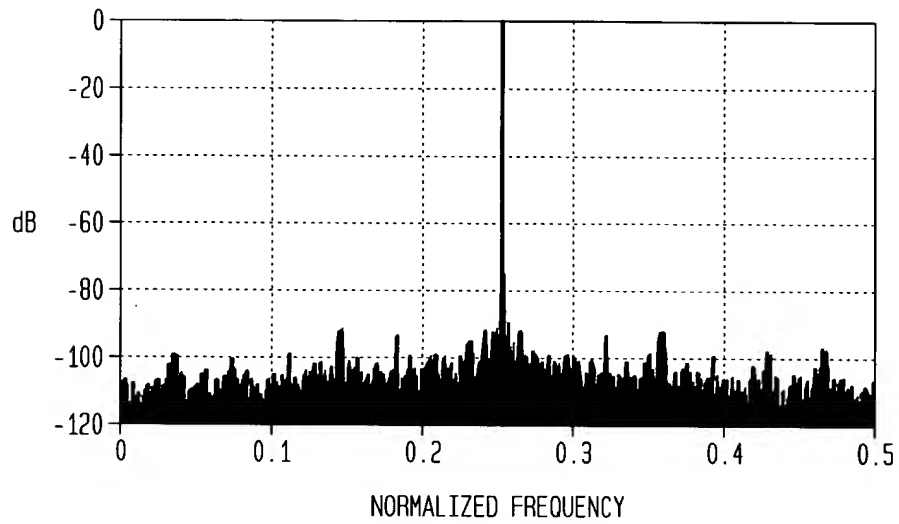
FIG. 41



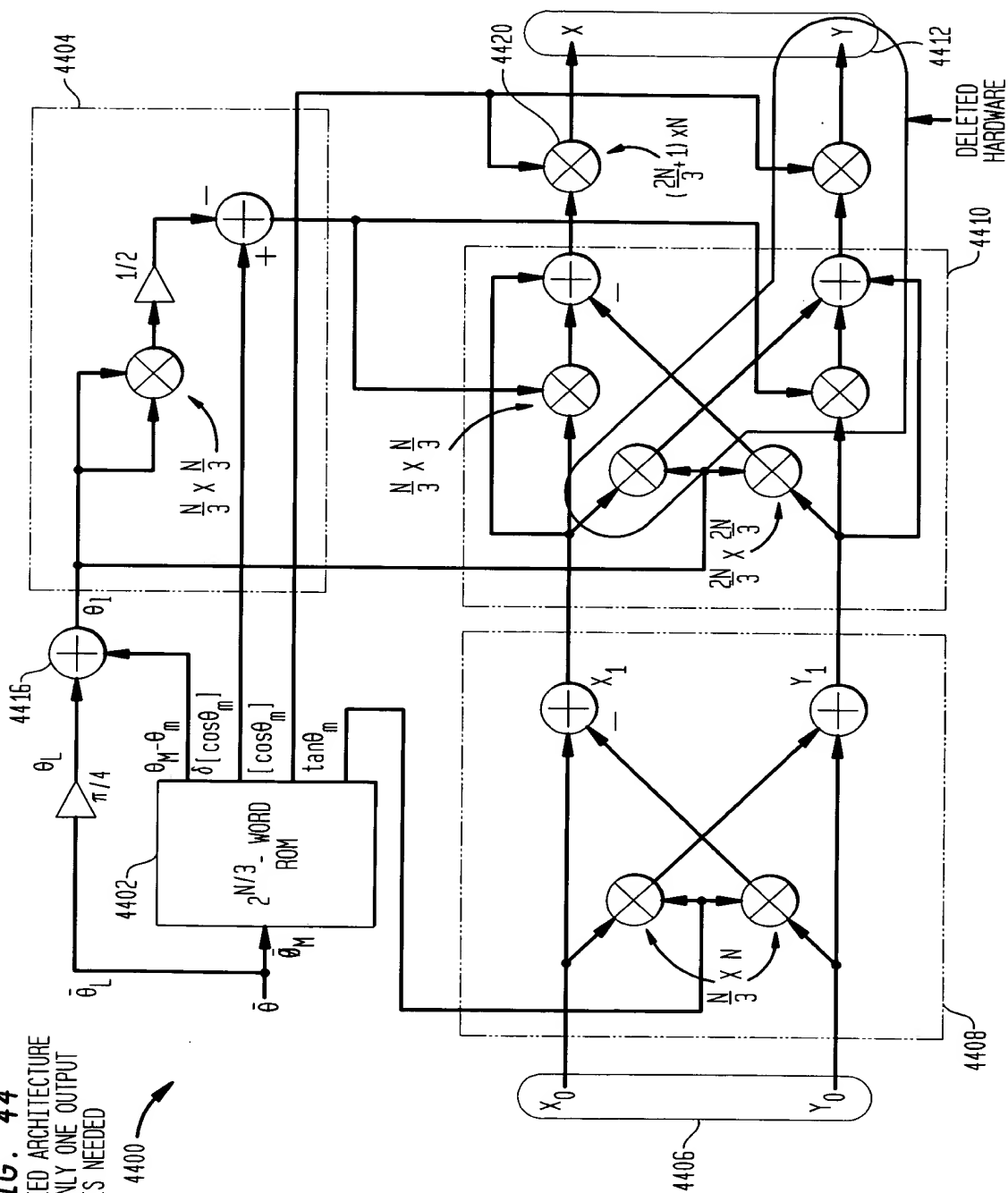


36/64

**FIG. 43**  
OUTPUT SPECTRUM SHOWING 90.36 dB SFDR

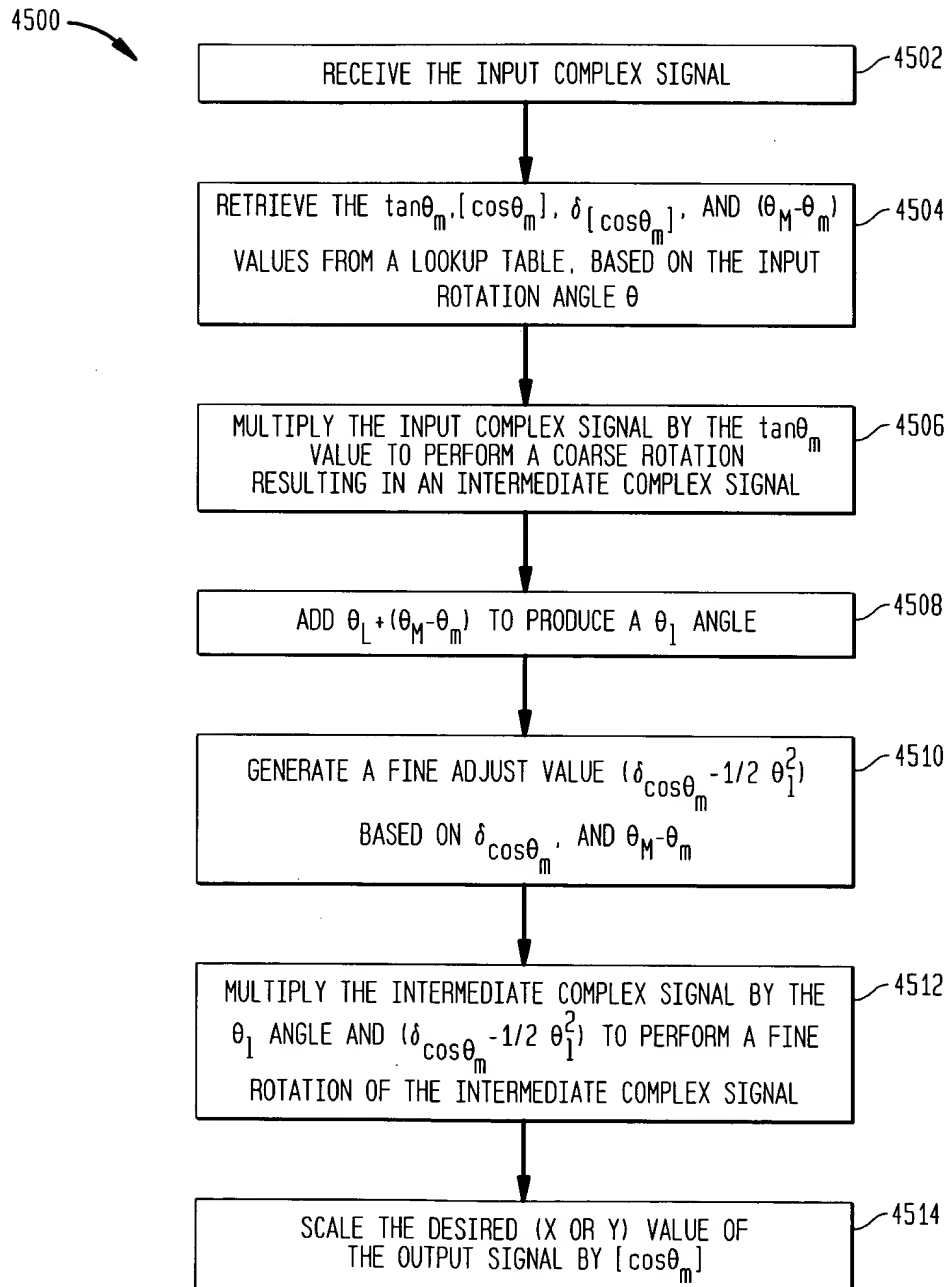


4400 



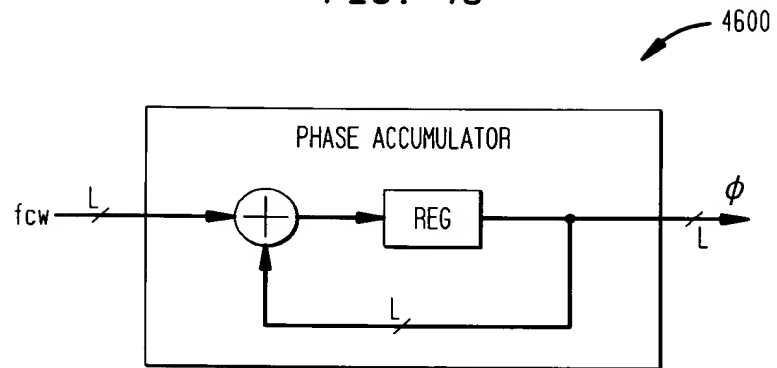
38/64

FIG. 45



39/64

FIG. 46



WHERE THE ADDER IS AN OVERFLOWING ACCUMULATOR

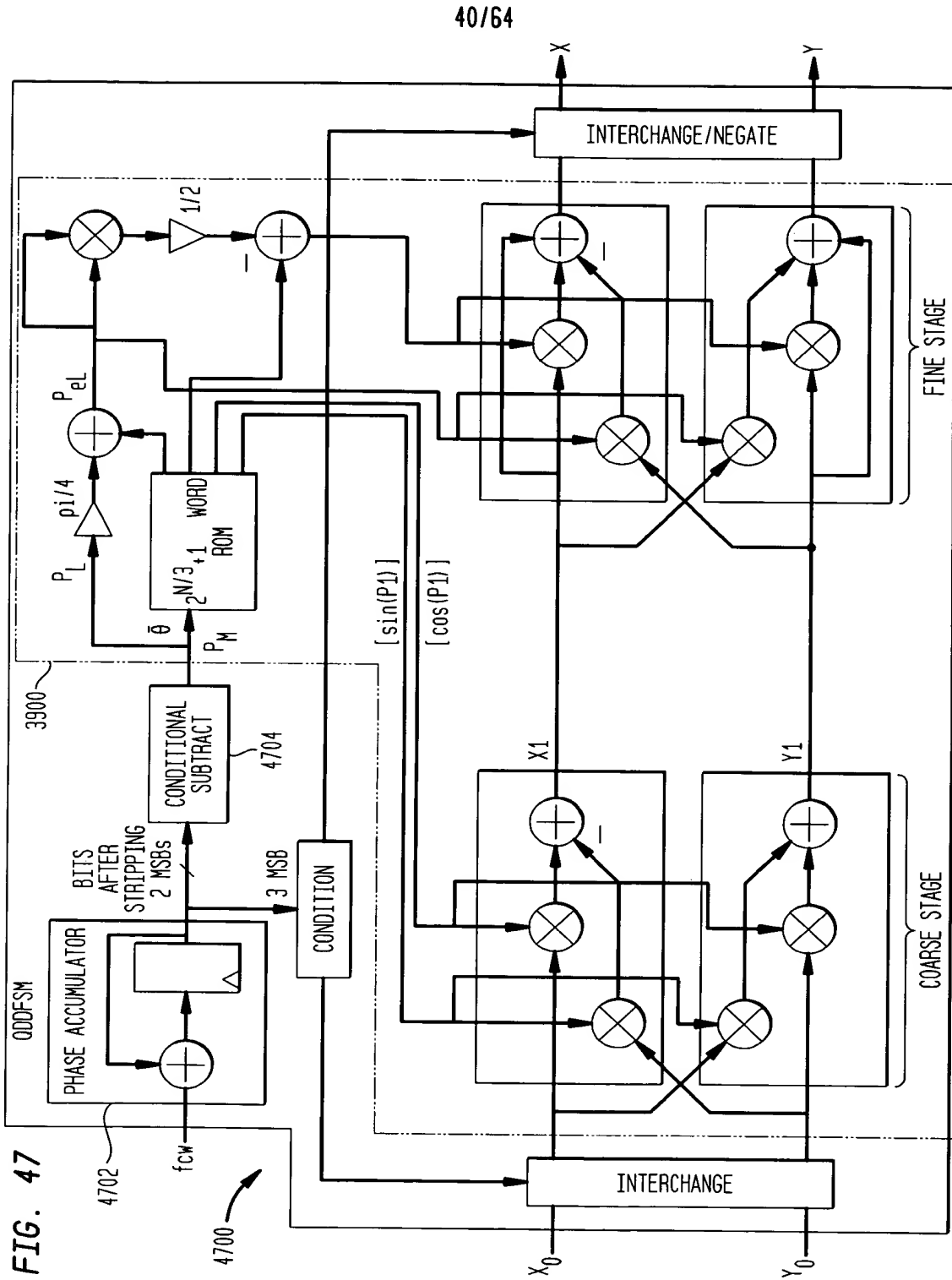


FIG. 47



41/64

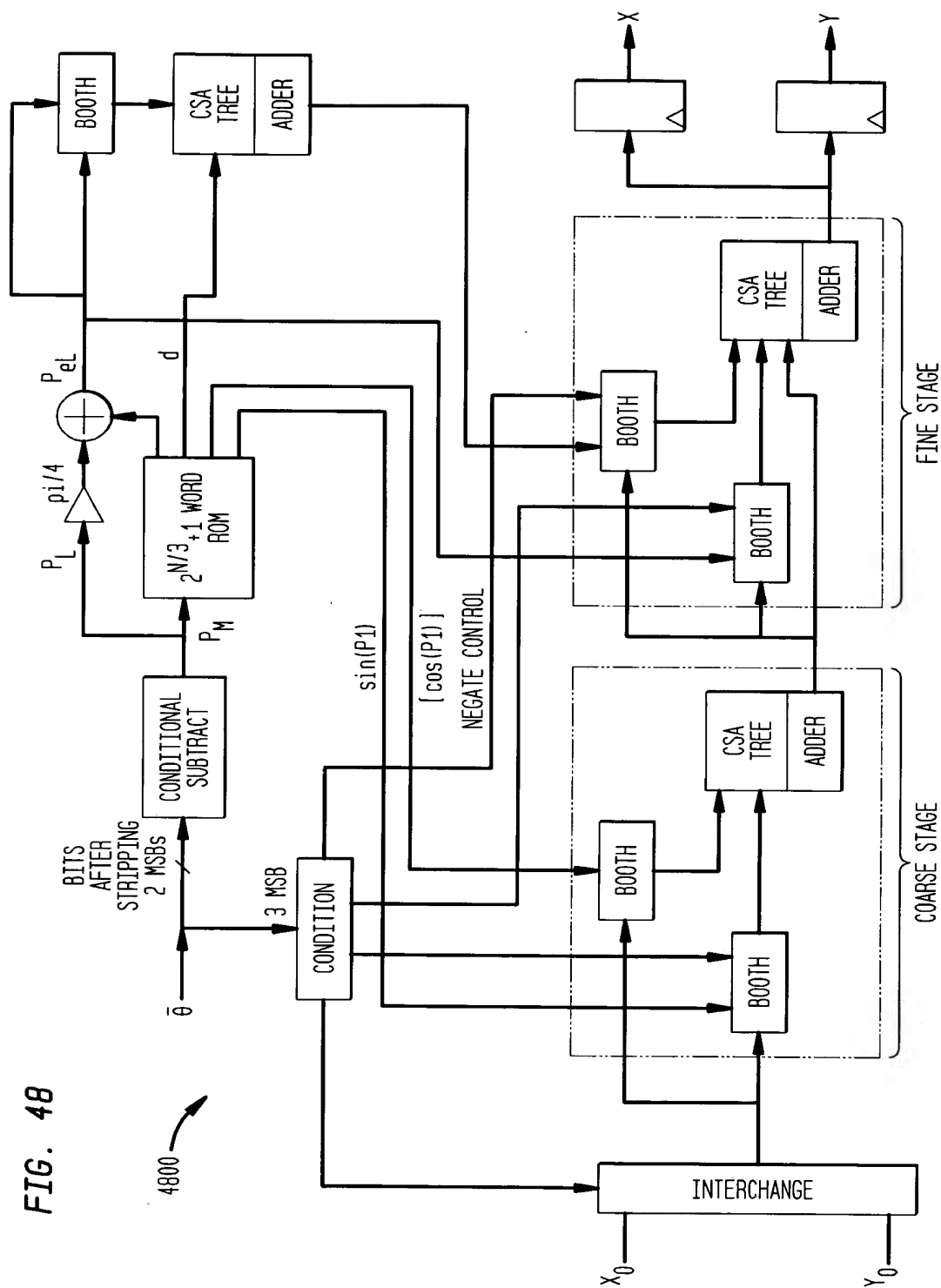
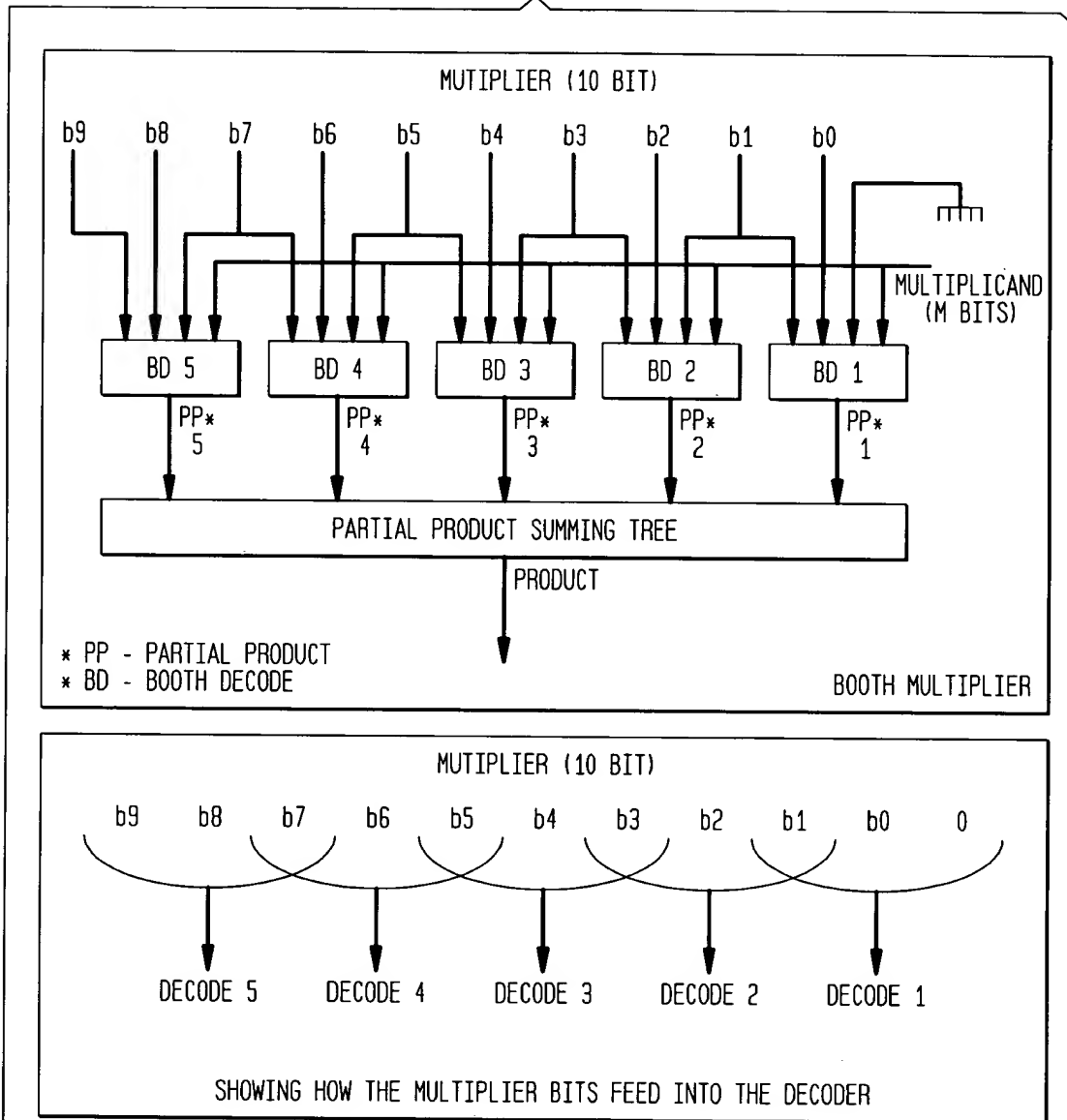


FIG. 48

42/64

FIG. 49



43/64

5000 **FIG. 50**

ORIGINAL BOOTH TABLE

5002

b2	b1	b0	PP
0	0	0	0*A
0	0	1	1*A
0	1	0	1*A
0	1	1	2*A
1	0	0	-2*A
1	0	1	-1*A
1	1	0	-1*A
1	1	1	0*A

5100 **FIG. 51**

NEGATING BOOTH TABLE

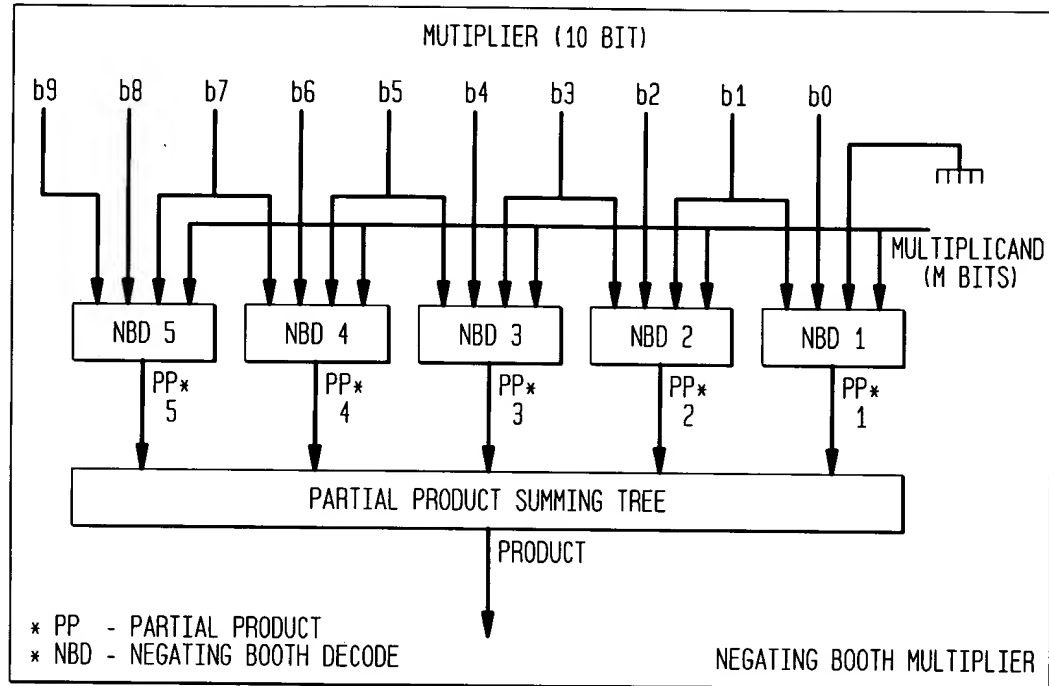
5102

b2	b1	b0	PP
0	0	0	0*A
0	0	1	-1*A
0	1	0	-1*A
0	1	1	-2*A
1	0	0	2*A
1	0	1	1*A
1	1	0	1*A
1	1	1	0*A

44/64

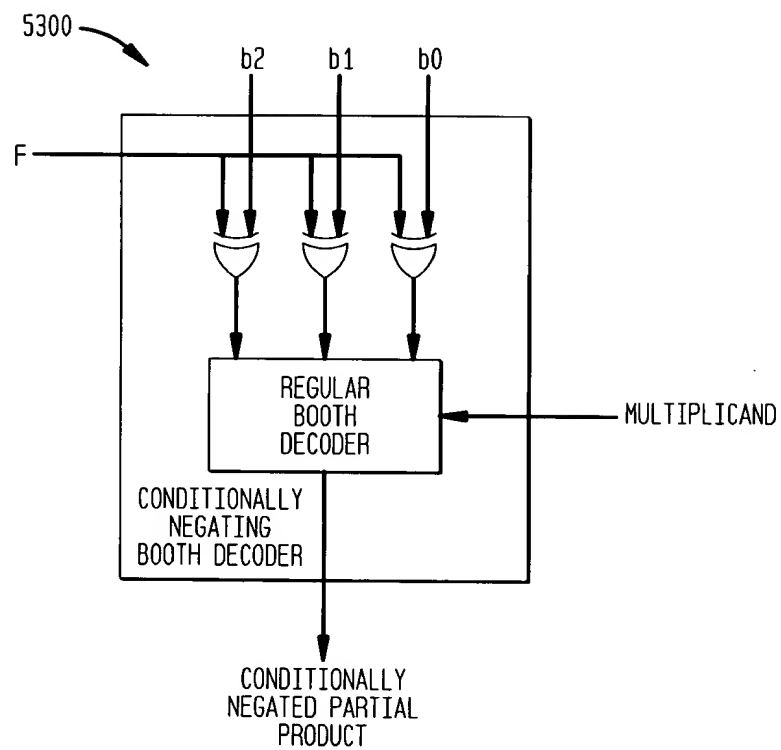
FIG. 52

5200



45/64

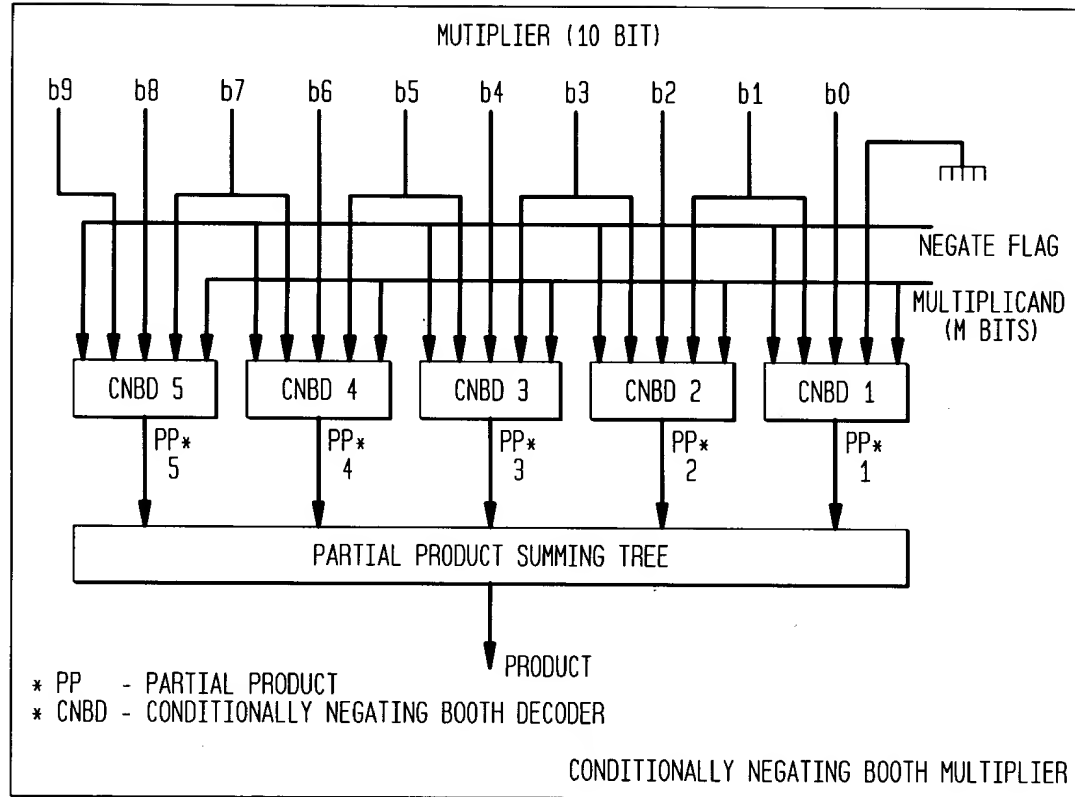
FIG. 53



46/64

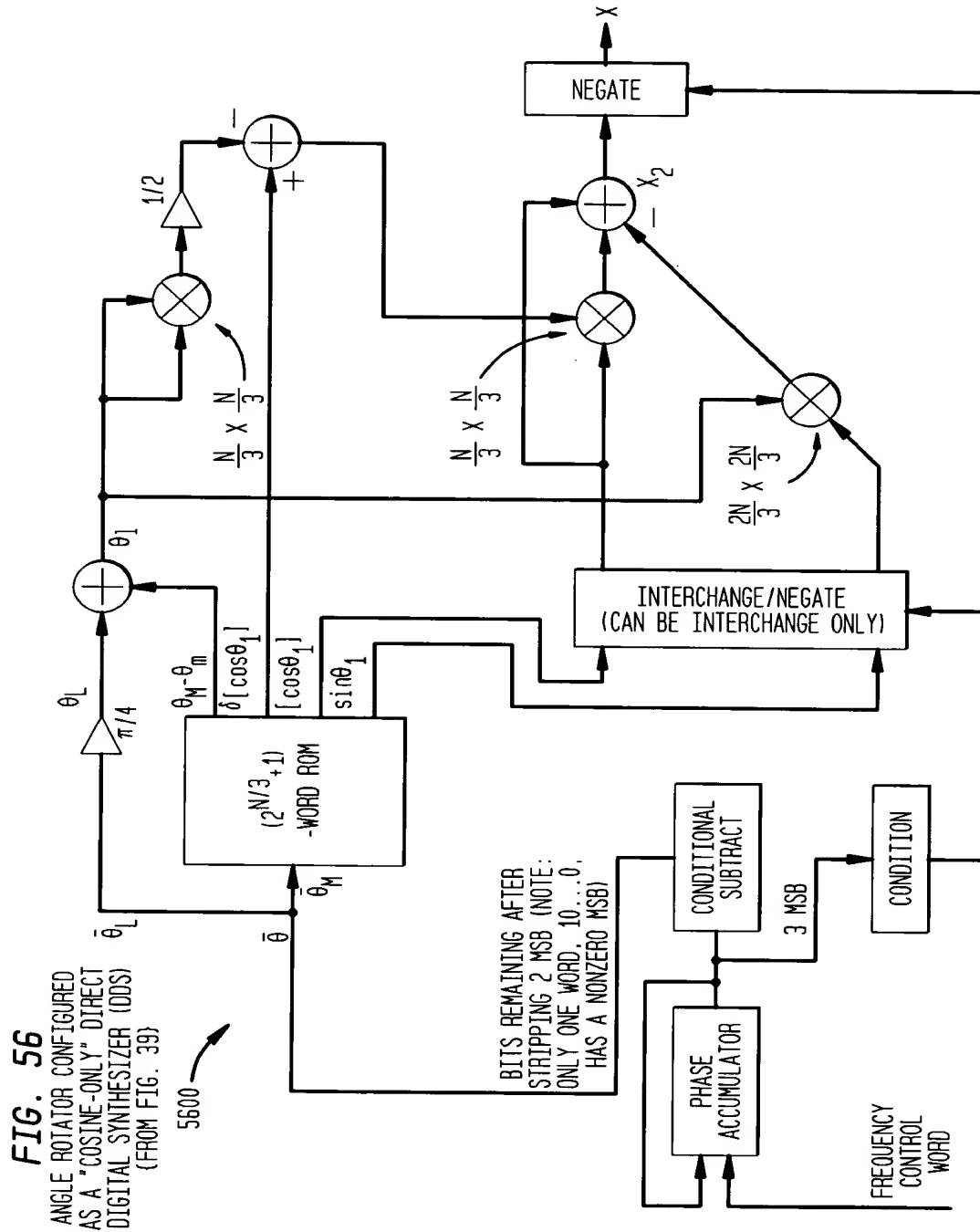
FIG. 54

5400





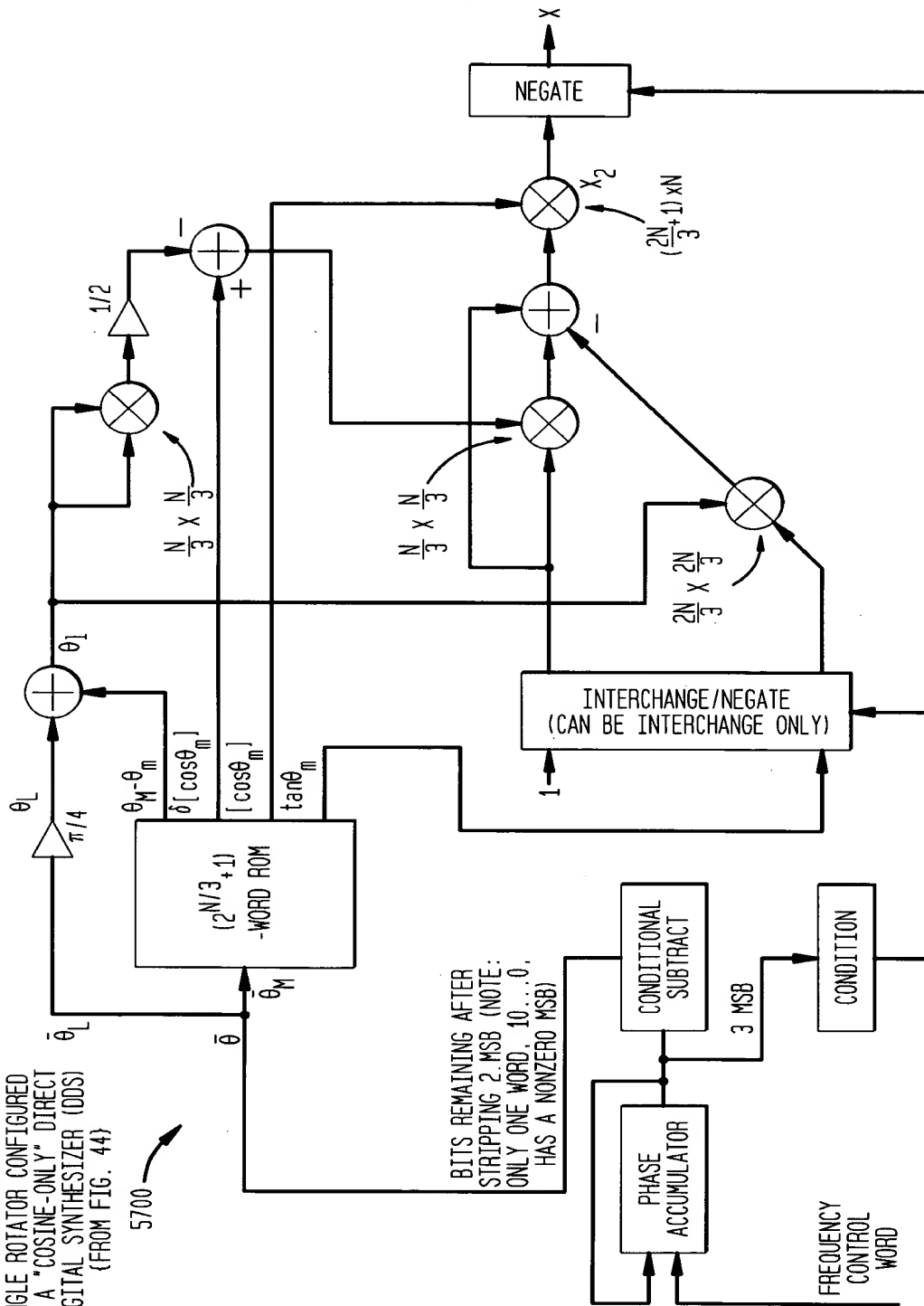
48/64





49/64

**FIG. 57**  
 ANGLE ROTATOR CONFIGURED  
 AS A "COSINE-ONLY" DIRECT  
 DIGITAL SYNTHESIZER (DDS)  
 (FROM FIG. 44)

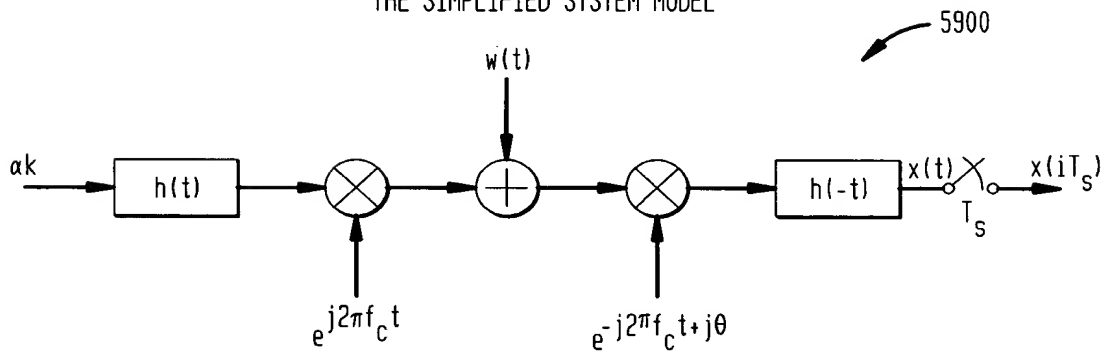


50/64

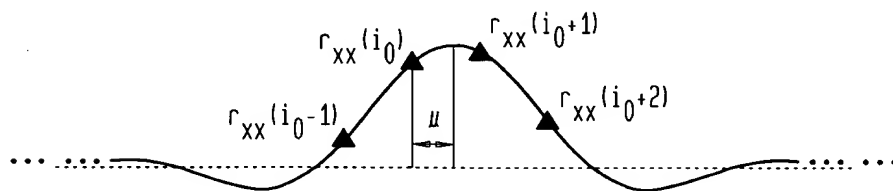
**FIG. 58**  
 COMMON PACKET FORMAT



**FIG. 59**  
 THE SIMPLIFIED SYSTEM MODEL

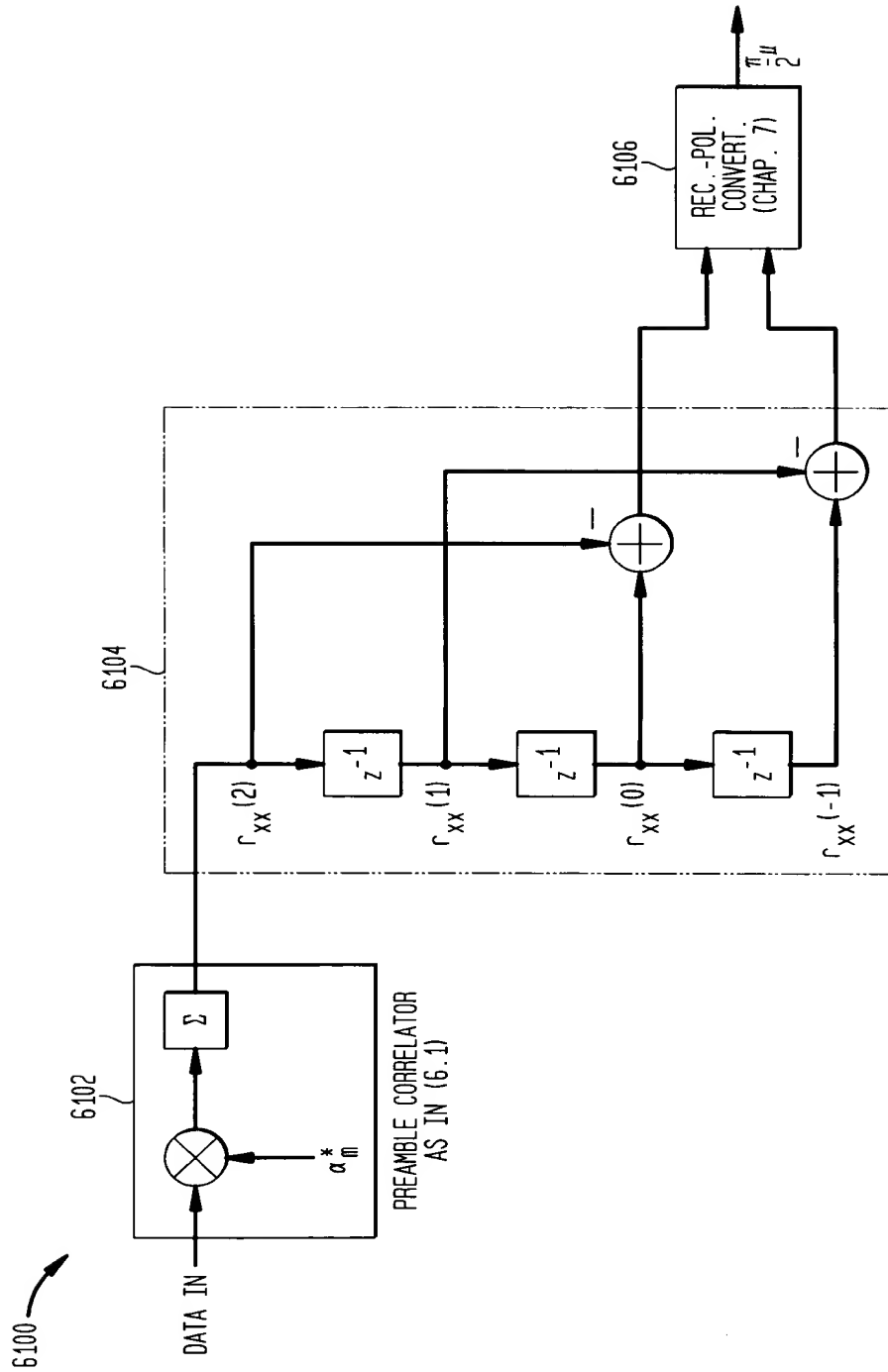


**FIG. 60**  
 MEAN VALUES OF THE PREAMBLE CORRELATOR OUTPUT, FOR  $\theta=0$



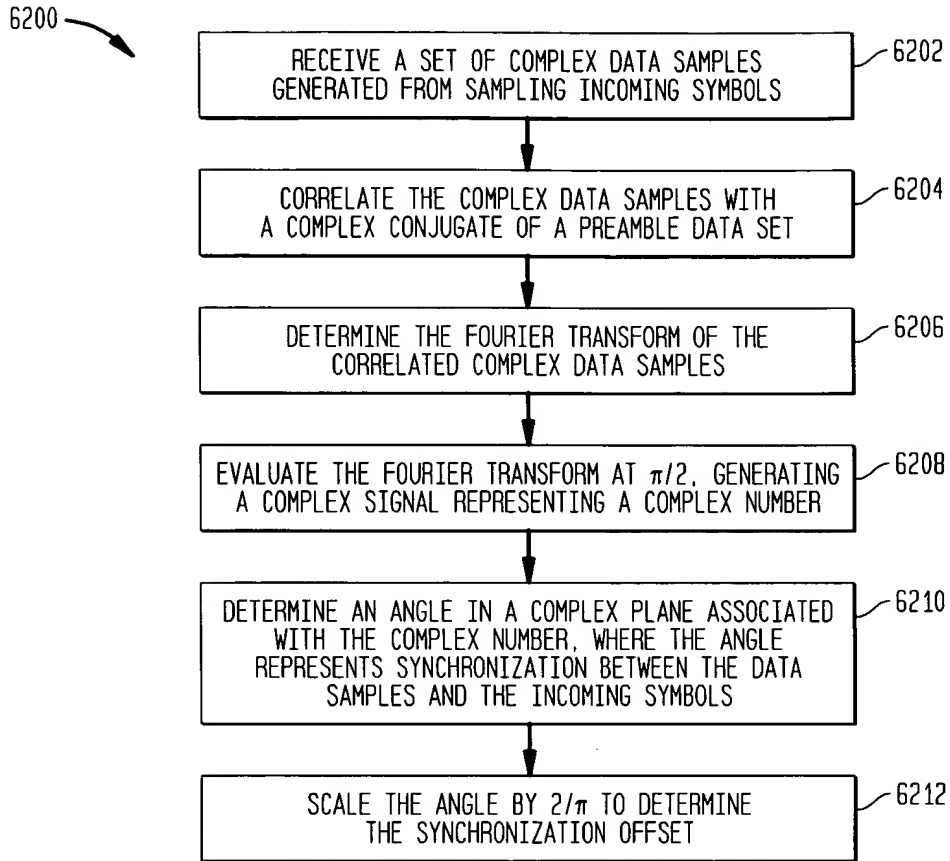
51/64

**FIG. 61**  
 PRELIMINARY SYMBOL-TIMING ESTIMATION STRUCTURE



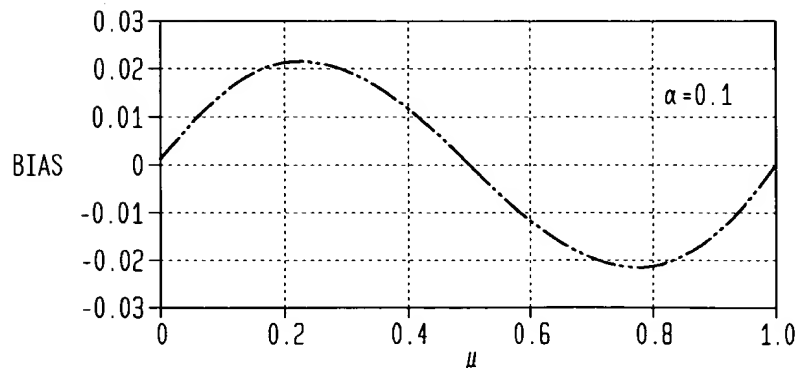
52/64

**FIG. 62**



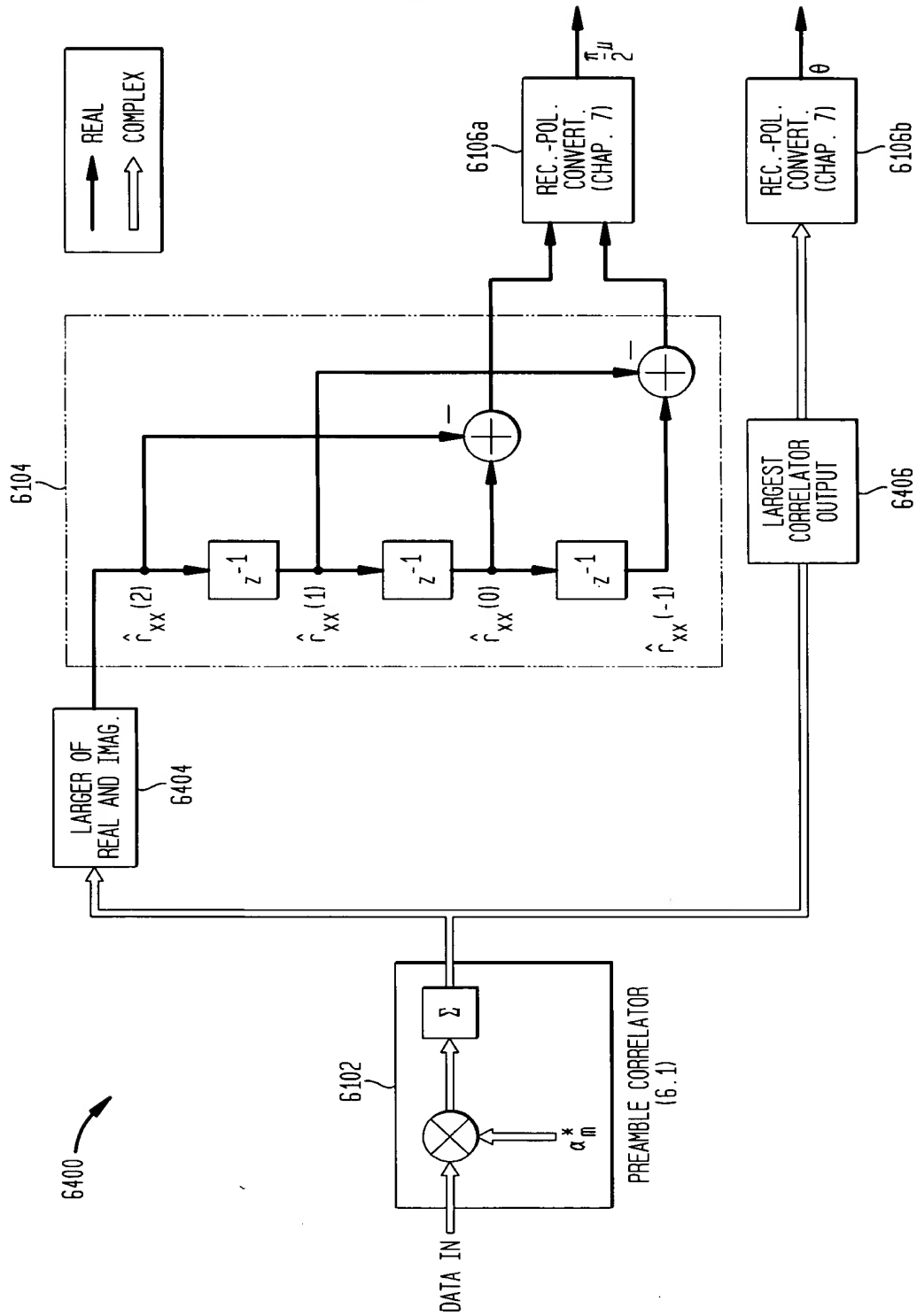
**FIG. 63**

BIAS DUE TO TRUNCATION



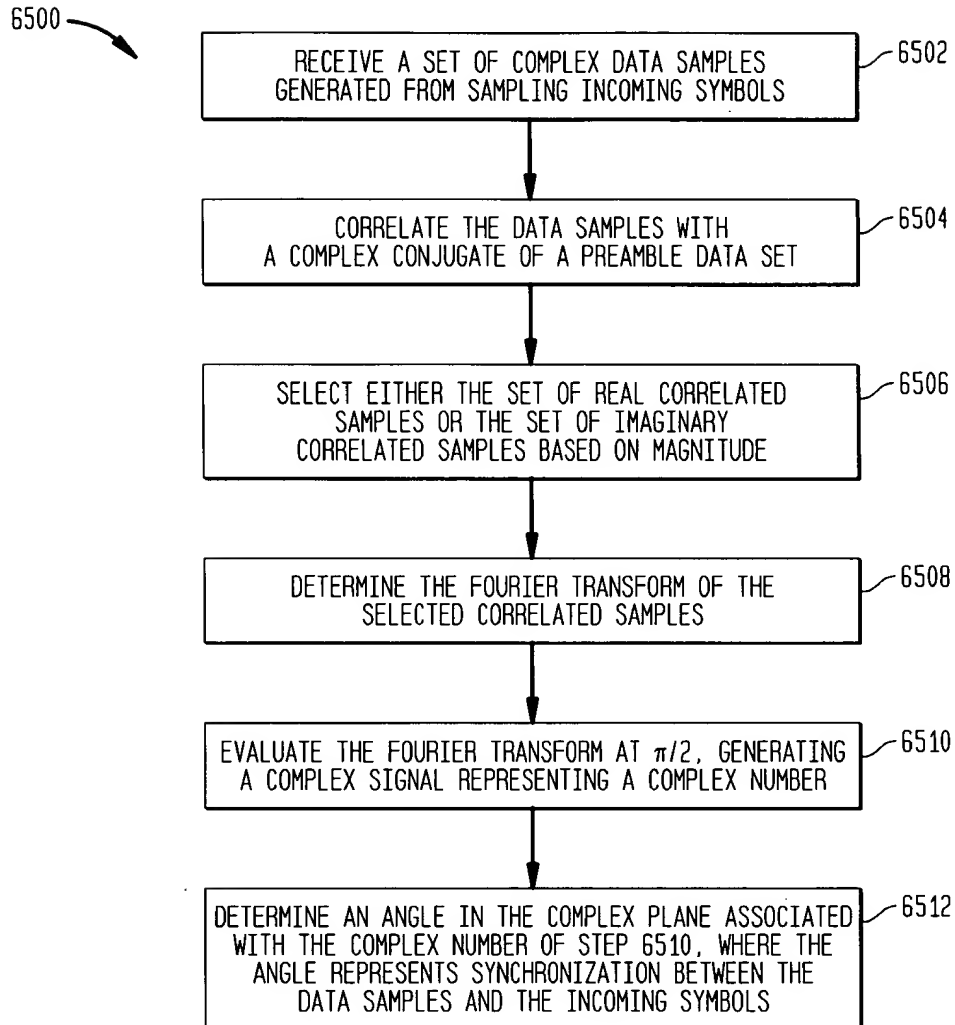
53/64

**FIG. 64**  
 STRUCTURE FOR CARRIER-PHASE AND SYMBOL TIMING RECOVERY



54/64

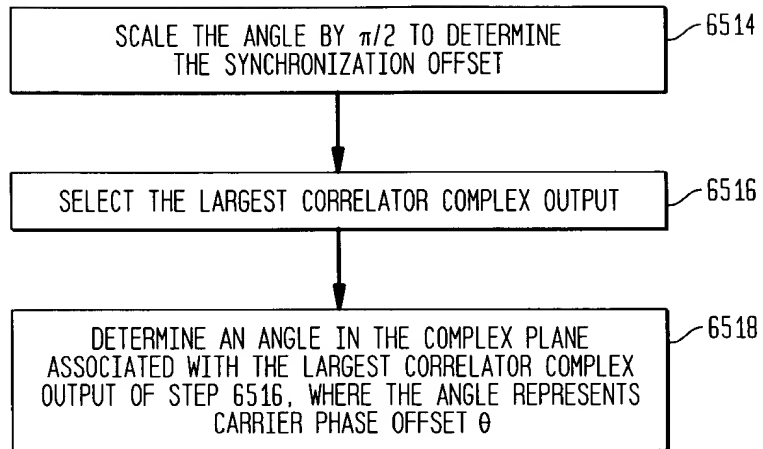
**FIG. 65A**



55/64

6500 (CONT.)

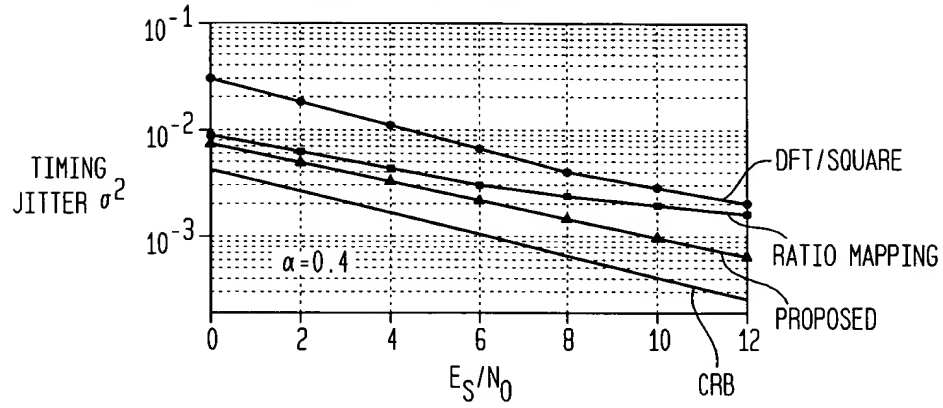
**FIG. 65B**



56/64

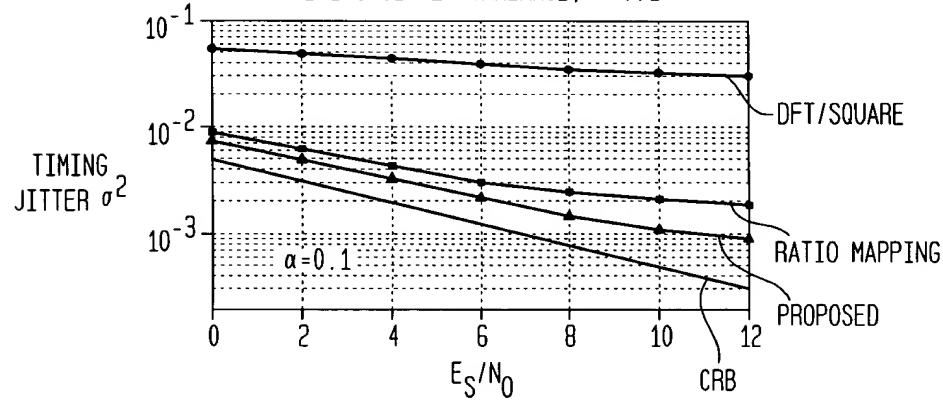
**FIG. 66**

TIMING JITTER VARIANCE,  $\alpha=0.4$



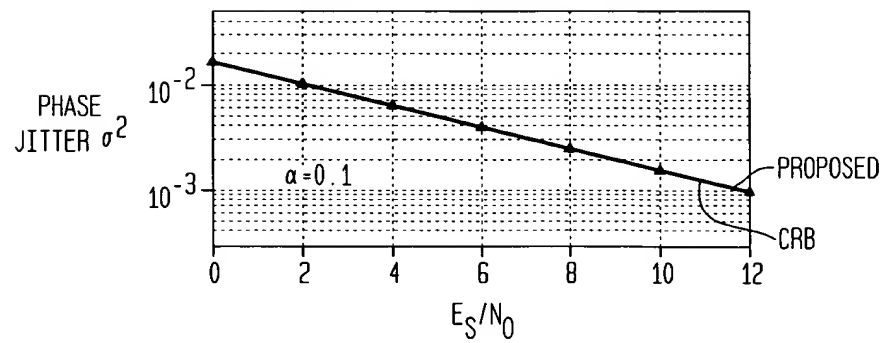
**FIG. 67**

TIMING JITTER VARIANCE,  $\alpha=0.1$



**FIG. 68**

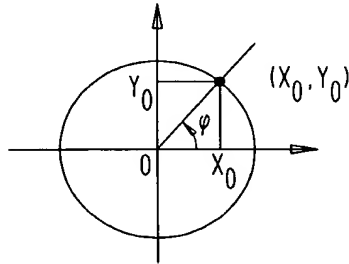
PHASE JITTER VARIANCE,  $\alpha=0.1$



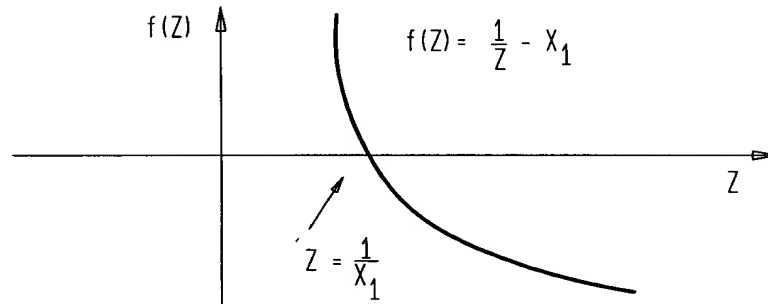


57/64

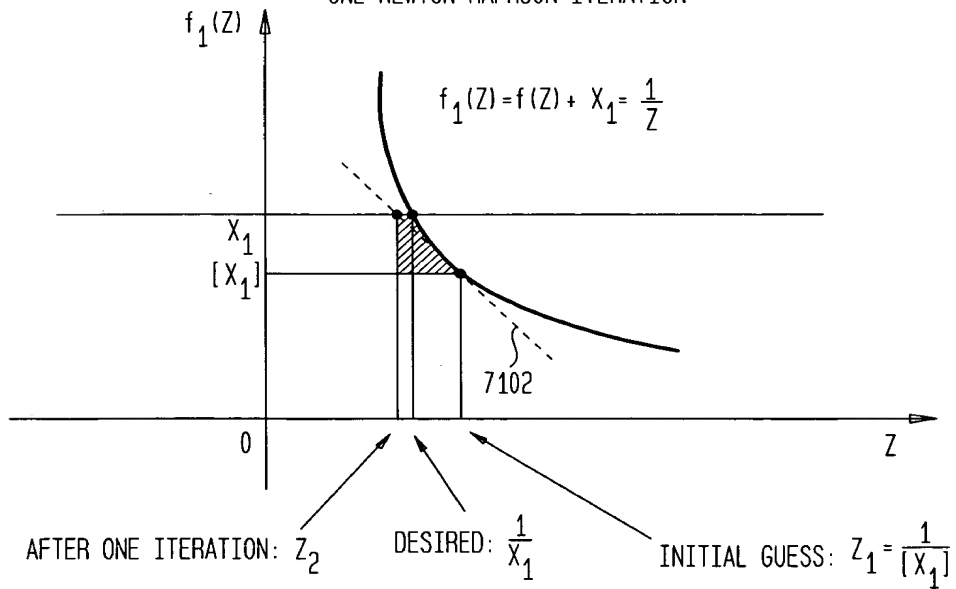
**FIG. 69**  
 CARTESIAN TO POLAR CONVERSION



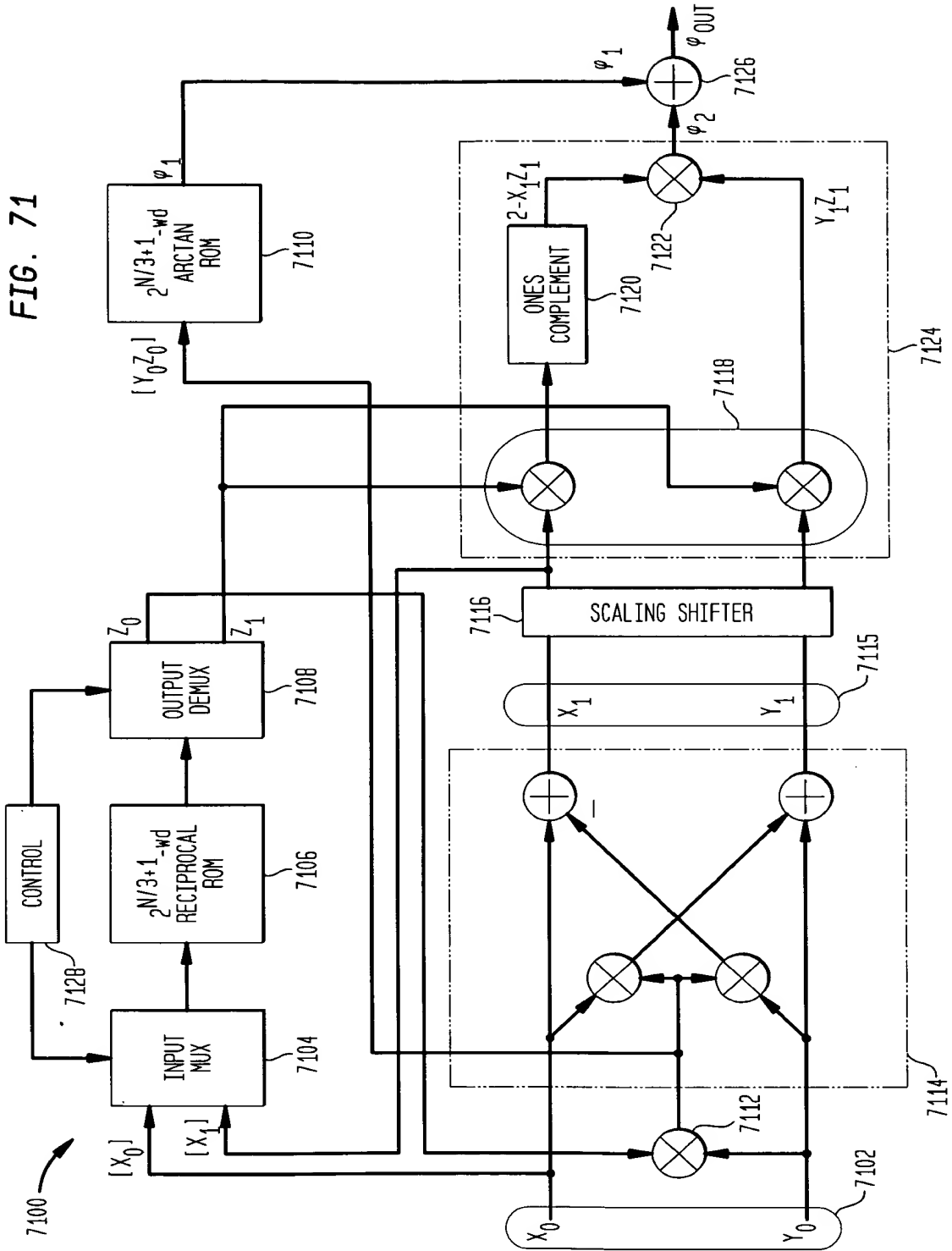
**FIG. 70A**  
 USING NEWTON-RAPHSON ITERATION TO FIND  $1/X_1$



**FIG. 70B**  
 ONE NEWTON-RAPHSON ITERATION

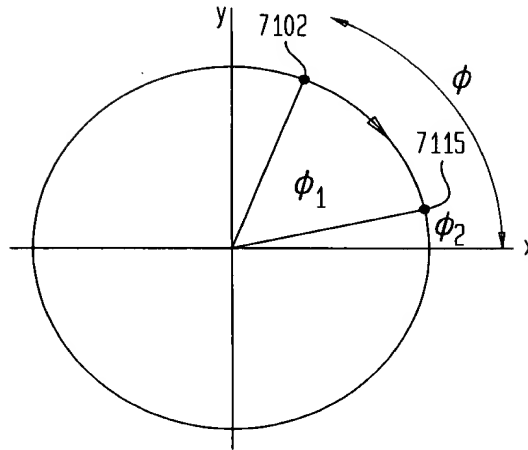


58/64



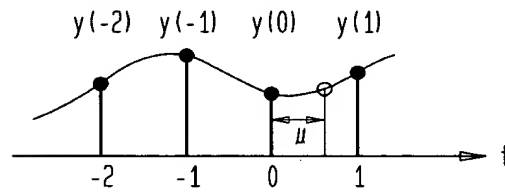
59/64

**FIG. 72**



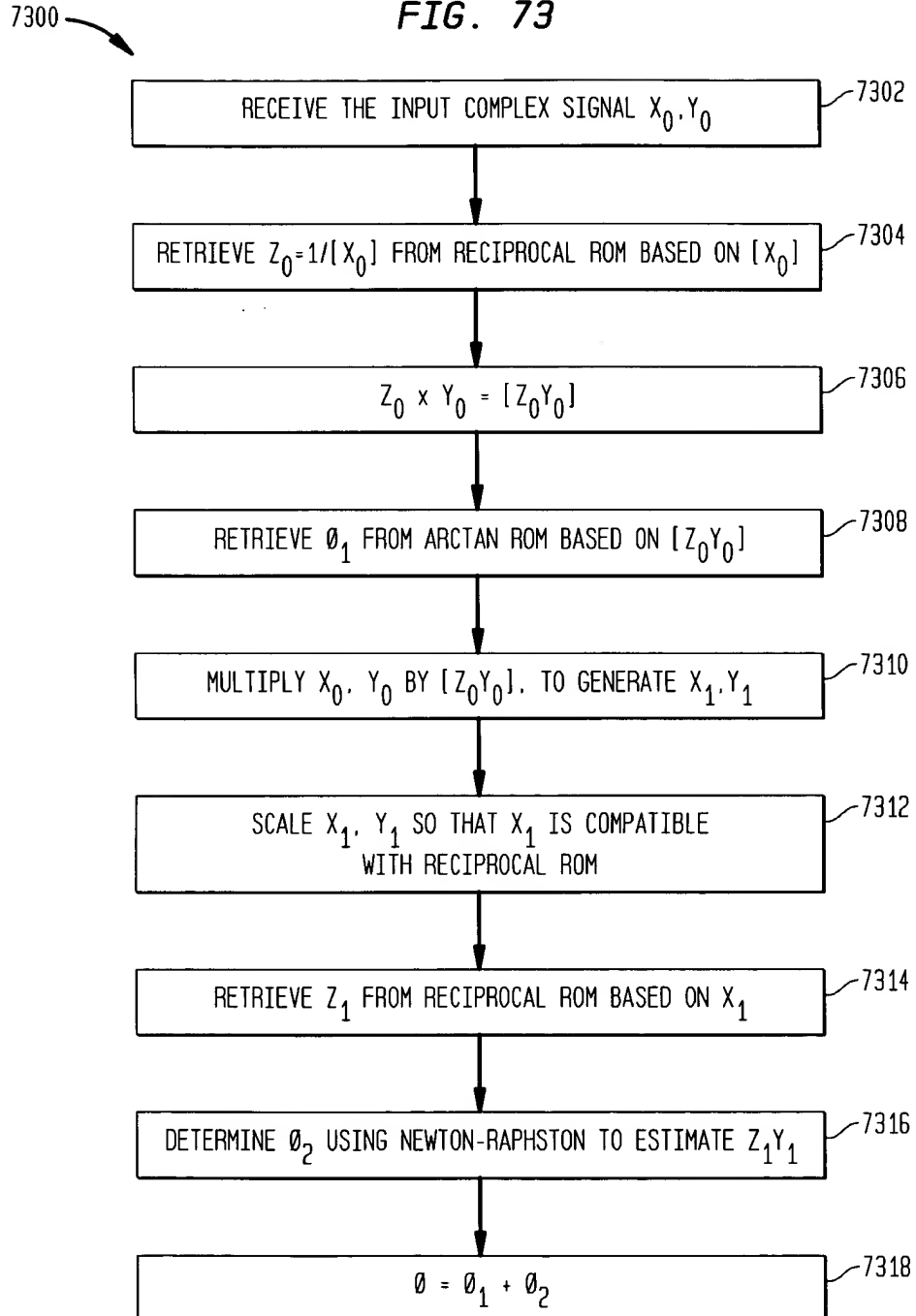
**FIG. 74**

INTERPOLATION IN A NON-CENTER INTERVAL



60/64

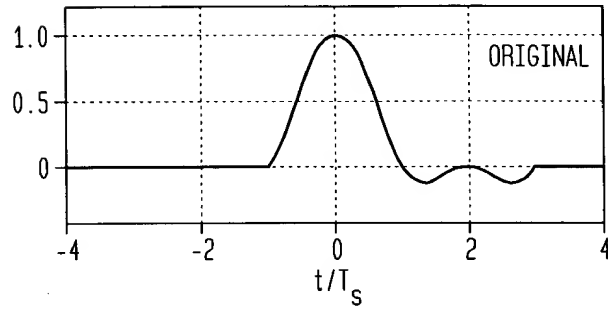
FIG. 73



61/64

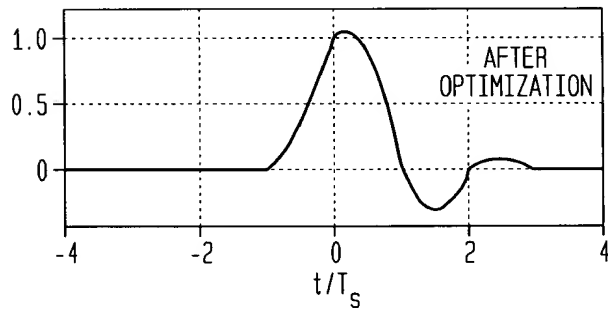
**FIG. 75A**

IMPULSE RESPONSES OF THE NON-CENTER-INTERVAL  
INTERPOLATION FILTER BEFORE OPTIMIZATION



**FIG. 75B**

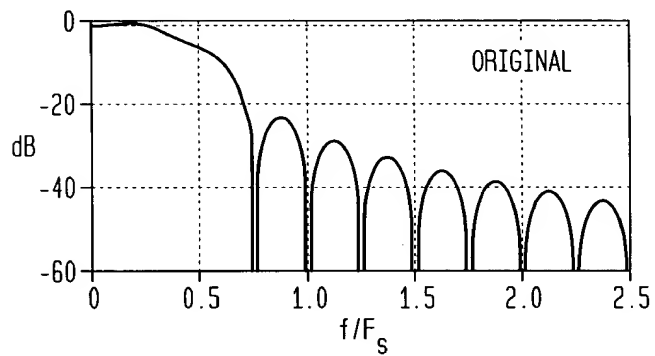
IMPULSE RESPONSES OF THE NON-CENTER-INTERVAL  
INTERPOLATION FILTER AFTER OPTIMIZATION



62/64

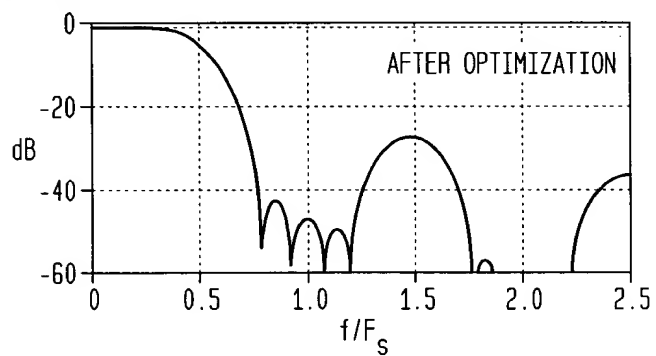
**FIG. 76A**

FREQUENCY RESPONSES OF THE NON-CENTER-INTERVAL INTERPOLATOR BEFORE OPTIMIZATION



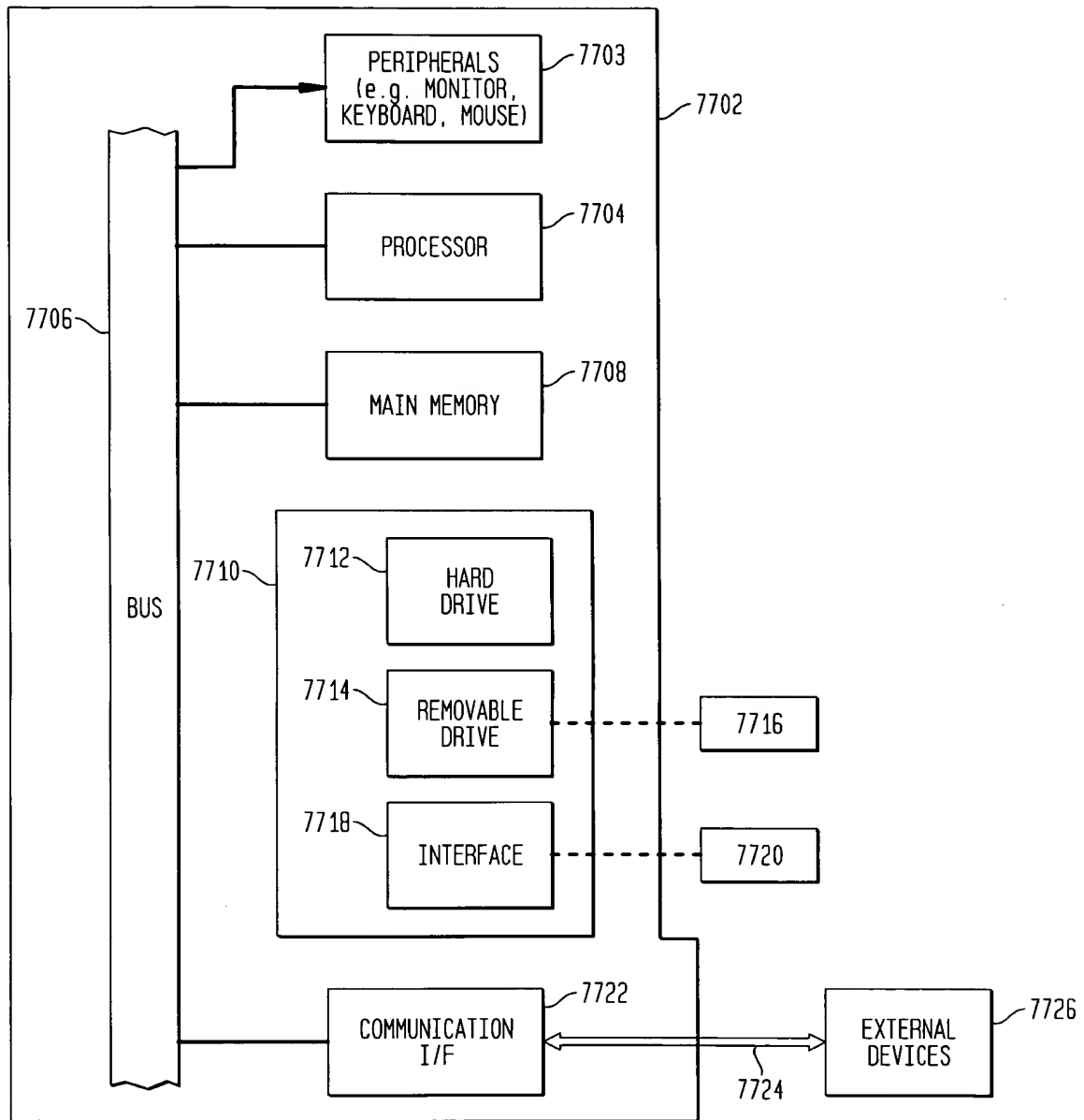
**FIG. 76B**

FREQUENCY RESPONSES OF THE NON-CENTER-INTERVAL INTERPOLATOR AFTER OPTIMIZATION



63/64

FIG. 77



64/64

**FIG. 78**  
 DATA RATE EXPANSION CIRCUIT

